Propofol attenuates cerebral ischemia–reperfusion-mediated neuronal apoptosis and oxidative damage by regulating the miR-6838-5p/AQP11 axis

XiuQin Wang[1]*, Liang Zhao[2], YangYang Shen[1], YongLai Zhang[1]

[1]Department of Anesthesiology, Shandong Cancer Hospital and Institute, Shandong First Medical University and Shandong Academy of Medical Sciences, China
[2]Department of Anesthesiology, The 960th Hospital of the PLA, China

Submitted: 21 November 2024; **Accepted:** 10 February 2025
Online publication: 20 April 2025

Arch Med Sci
DOI: https://doi.org/10.5114/aoms/201185

***Corresponding author:**
XiuQin Wang
Department of Anesthesiology
Shandong Cancer Hospital and Institute
Shandong First Medical University and Shandong Academy of Medical Sciences
China
E-mail: wangxiuqin829@hotmail.com

Abstract

Introduction: This study aimed to elucidate the mechanism by which propofol (PPF) exerts its effects in cerebral ischemia–reperfusion injury (CI/RI).
Material and methods: A rat model of CI/RI was established via middle cerebral artery occlusion/reperfusion (MCAO/R). MCAO/R rats were pre-treated with PPF (10 mg/kg) via intraperitoneal injection. Additionally, 48 h before PPF administration, miR-6838-5p agomir/antagomir and aquaporin-11 (AQP11) lentiviral overexpression vectors were injected into MCAO/R rats. Infarct size was determined using 2,3,5-triphenyl tetrazolium chloride staining. Neurological function was assessed using standardized scoring, and cerebral edema was measured by determining brain water content. Hematoxylin-eosin staining, Nissl staining, and terminal deoxynucleotidyl transferase dUTP nick end labeling staining were performed on brain tissues. Inflammatory and oxidative markers were evaluated. A hypoxia/reoxygenation (H/R) injury model was established in PC12 cells to assess miR-6838-5p and AQP11 expression levels, as well as cell viability and apoptosis.
Results: The lethal dose 50 (LD_{50}) of PPF in rats was determined to be 22.6 mg/kg, significantly higher than the therapeutic dose. PPF or overexpression of miR-6838-5p resulted in reduced cerebral infarct size, neuronal necrosis, and apoptosis, increased Nissl bodies, and decreased brain edema, apoptosis, tumor necrosis factor-α, interleukin-1β, and malondialdehyde (MDA) levels. Glutathione peroxidase (GSH-Px) and superoxide dismutase (SOD) activities were elevated in MCAO/R rats treated with PPF. These protective effects of PPF were reversed by miR-6838-5p knockdown or AQP11 overexpression. PPF ameliorated H/R-induced neuronal damage, enhanced neuronal activity, reduced apoptosis and MDA production, and increased GSH-Px and SOD levels.
Conclusions: PPF ameliorates CI/RI by modulating the miR-6838-5p/AQP11 axis.

Key words: middle cerebral artery occlusion/reperfusion, anesthetic, miRNA, stroke, cerebral infarction.

Introduction

Ischemic stroke is a major cause of morbidity and mortality, leading to a range of complications such as cognitive impairment and epilepsy [1, 2]. With its increasing prevalence worldwide, ischemic stroke represents

a significant public health burden, contributing to long-term disability and reduced quality of life among survivors [3]. Cerebral ischemia–reperfusion injury (CI/RI) occurs when blood supply returns to ischemic brain tissue, typically during the treatment of ischemic stroke [4, 5]. CI/RI involves multiple pathophysiological mechanisms, including inflammation, oxidative stress, accumulation of metabolic toxins, and apoptosis, which collectively exacerbate brain injury [6, 7]. Current therapeutic strategies, which mainly aim to restore blood flow via thrombolysis or mechanical thrombectomy, are often limited by narrow therapeutic windows and the risk of adverse effects, highlighting the urgent need for adjunctive treatments that can mitigate the damaging consequences of reperfusion [8]. Despite extensive research, effective treatments for CI/RI remain elusive, making the exploration of its pathogenesis and the development of therapeutic interventions critical [9].

Propofol (PPF), a 2,6-diisopropylphenol-based intravenous general anesthetic, is widely used for anesthesia and sedation. Beyond its anesthetic properties, PPF shows multiple pharmacological effects, which encompass antioxidant, anti-inflammatory, and neuroprotective functions [10, 11], which make it a promising candidate for therapeutic intervention in CI/RI. Beyond its anesthetic properties, PPF possesses antioxidant, anti-inflammatory, and neuroprotective effects [12, 13]. Increasing preclinical evidence indicates that PPF offers pharmacological benefits in various diseases, including cardiovascular and cerebrovascular disorders [14–16], cancer [17], and neurodegenerative diseases [18, 19]. Notably, several studies have demonstrated that PPF pretreatment can mitigate CI/RI-induced brain damage by attenuating oxidative stress and apoptosis [20–23]. Nonetheless, the specific molecular processes responsible for these protective effects are not well understood. Recent research has revealed that PPF may exert its neuroprotective effects through epigenetic regulation, particularly by altering the expression patterns of microRNAs (miRNAs), which are crucial post-transcriptional regulators during ischemic injury. For instance, miR-6838-5p was reported to be downregulated in CI/RI and to protect the blood–brain barrier by targeting PDCD4 [24]. However, whether miR-6838-5p also affects CI/RI by regulating other downstream mRNAs remains to be further elucidated. Notably, AQP11, a member of the aquaporin (AQP) family, is a transmembrane protein that transports water and small solutes [25]. AQP11 has been found to be abundantly expressed in brain tissues, but its role and function in brain tissues are unknown [26]. Based on previous bioinformatics analysis, we identified a potential binding site for miR-6838-5p and AQP11. Therefore, we hypothesized that miR-6838-5p might be involved in the CI/RI process by targeting AQP11.

This investigation sought to determine the effects of PPF on CI/RI and to explain its molecular mechanisms by employing a middle cerebral artery occlusion/reperfusion (MCAO/R) rat model and a hypoxia/reoxygenation (H/R) injury model in PC12 cells. Specifically, we focused on the role of the miR-6838-5p/AQP11 axis as a novel research target, potentially contributing to the neuroprotective effects of PPF in CI/RI.

Material and methods

Laboratory animals

A total of 240 specific pathogen-free male Sprague-Dawley (SD) rats (8–10 weeks old, 250 ±30 g) were obtained from Jinan Pengyue Animal Breeding Co., Ltd. The rats were kept under specific conditions (23 ±2°C, 55 ±5% humidity) with a 12-hour light/dark cycle and had unrestricted access to food and water. In order to minimize experimental bias and ensure the scientific validity and reliability of the results, all rats were assigned to different experimental groups or control groups according to the needs of the study by third-party staff unrelated to the subsequent operations using the random number table method prior to the experiment. At the same time, in order to prevent subjective interference and information bias, the experimental operators and data collectors were kept in ignorance of the information on grouping until after all operations and data recording had been completed, and then the grouping was blinded and statistically analyzed by a third party. All animal experiments were conducted in accordance with the National Institutes of Health (NIH) guidelines and were approved by the Animal Care and Use Committee of our Hospital (Approval Number: SDTHEC).

Rat MCAO/R model

An MCAO/R rat model was established using a surgical procedure as described previously [27]. Briefly, rats were anesthetized via intraperitoneal injection of 3% (w/v) pentobarbital sodium (40 mg/kg). The left internal carotid artery was exposed, and a 4/0 surgical nylon monofilament was inserted to occlude blood flow in the middle cerebral artery, internal carotid artery, anterior cerebral artery, and posterior cerebral artery. After 2 h of occlusion, the filament was withdrawn to allow reperfusion for 24 h. Body temperature was maintained at approximately 37°C throughout the procedure. No instances of post-anesthesia peritonitis or intestinal obstruction were observed. Rats in the sham group underwent the same surgical procedure without filament insertion.

Rat treatments

SD rats were randomly assigned to six groups (n = 6 per group), with PPF dosing adjusted based on body weight [28]:

- Sham Group (as a negative control for the MCAO/R group): rats underwent sham surgery and received an intraperitoneal injection of normal saline 10 minutes prior to surgery.
- MCAO/R Group: rats underwent MCAO/R and received an intraperitoneal injection of normal saline 10 min prior to surgery.
- MCAO/R + Dimethyl Sulfoxide (DMSO) Group (as a negative control for the MCAO/R + PPF group): rats underwent MCAO/R and received an intraperitoneal injection of 0.01% DMSO 10 min prior to surgery.
- MCAO/R + PPF Group: rats underwent MCAO/R and received an intraperitoneal injection of PPF (10 mg/kg; Xiyuan-Bio, Shanghai, China) 10 min prior to surgery [29, 30]. The chemical structure of PPF is illustrated in Figure 1 A.
- MCAO/R + agomiR-NC Group: After anesthesia, rats were injected with agomiR-NC prior to MCAO/R.
- MCAO/R + agomiR-miR-6838-5p Group: After anesthesia, rats were injected with agomiR-miR-6838-5p prior to MCAO/R.

Additional groups included combinations of PPF with antagomirs and lentiviral vectors:

- MCAO/R + PPF + anta-NC Group: After anesthesia, rats were injected with antagomir-NC. After 48 h, rats received an intraperitoneal injection of PPF (10 mg/kg) and underwent MCAO/R.
- MCAO/R + PPF + anta-miR-6838-5p Group: After anesthesia, rats were injected with antagomir-miR-6838-5p. After 48 h, rats received an intraperitoneal injection of PPF (10 mg/kg) and underwent MCAO/R.
- MCAO/R + PPF + LV-NC Group: After anesthesia, rats were injected with antagomir-miR-6838-5p and LV-NC. After 48 h, rats received an intraperitoneal injection of PPF (10 mg/kg) and underwent MCAO/R.
- MCAO/R + PPF + LV-AQP11 Group: After anesthesia, rats were injected with antagomir-miR-6838-5p and LV-AQP11. After 48 h, rats received an intraperitoneal injection of PPF (10 mg/kg) and underwent MCAO/R.

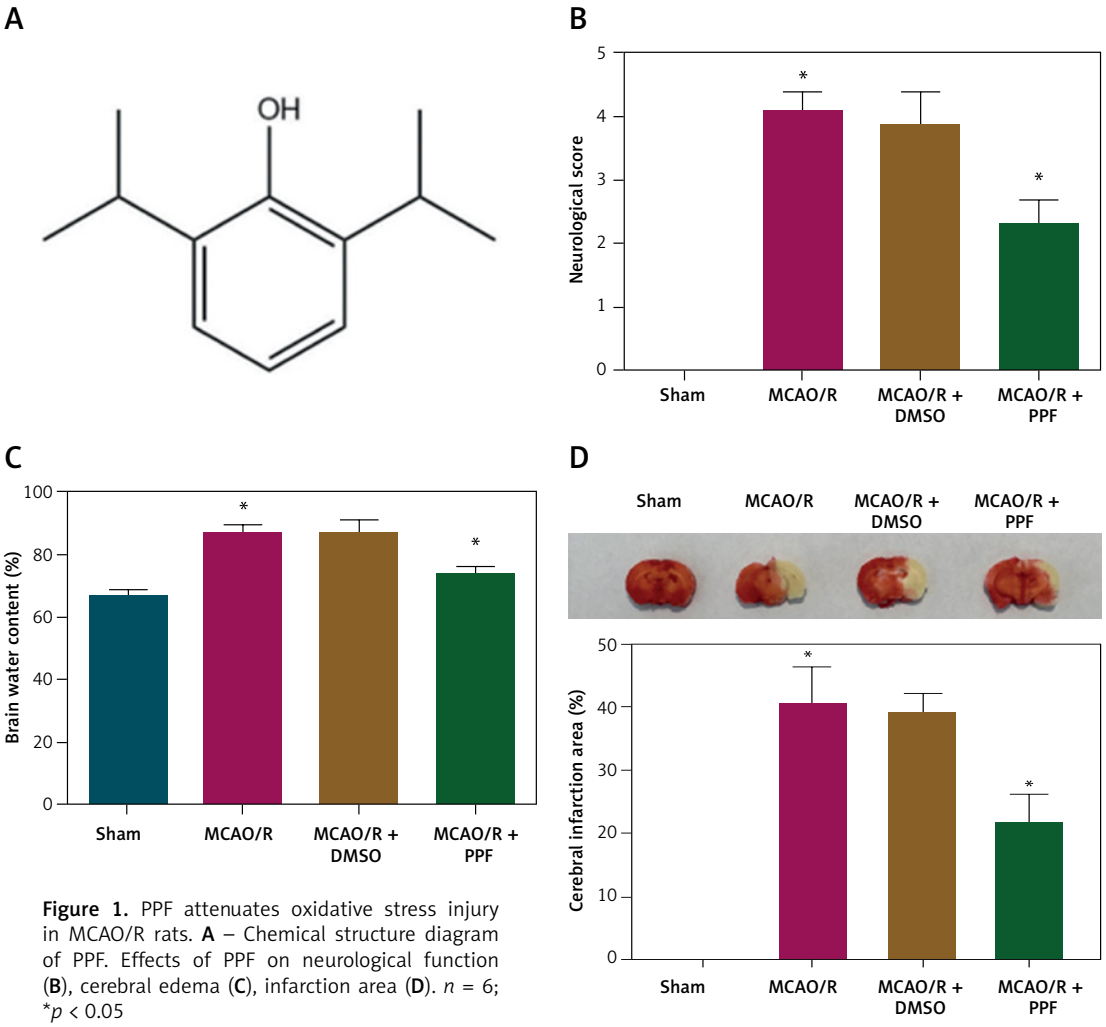

Figure 1. PPF attenuates oxidative stress injury in MCAO/R rats. **A** – Chemical structure diagram of PPF. Effects of PPF on neurological function (**B**), cerebral edema (**C**), infarction area (**D**). n = 6; *p < 0.05

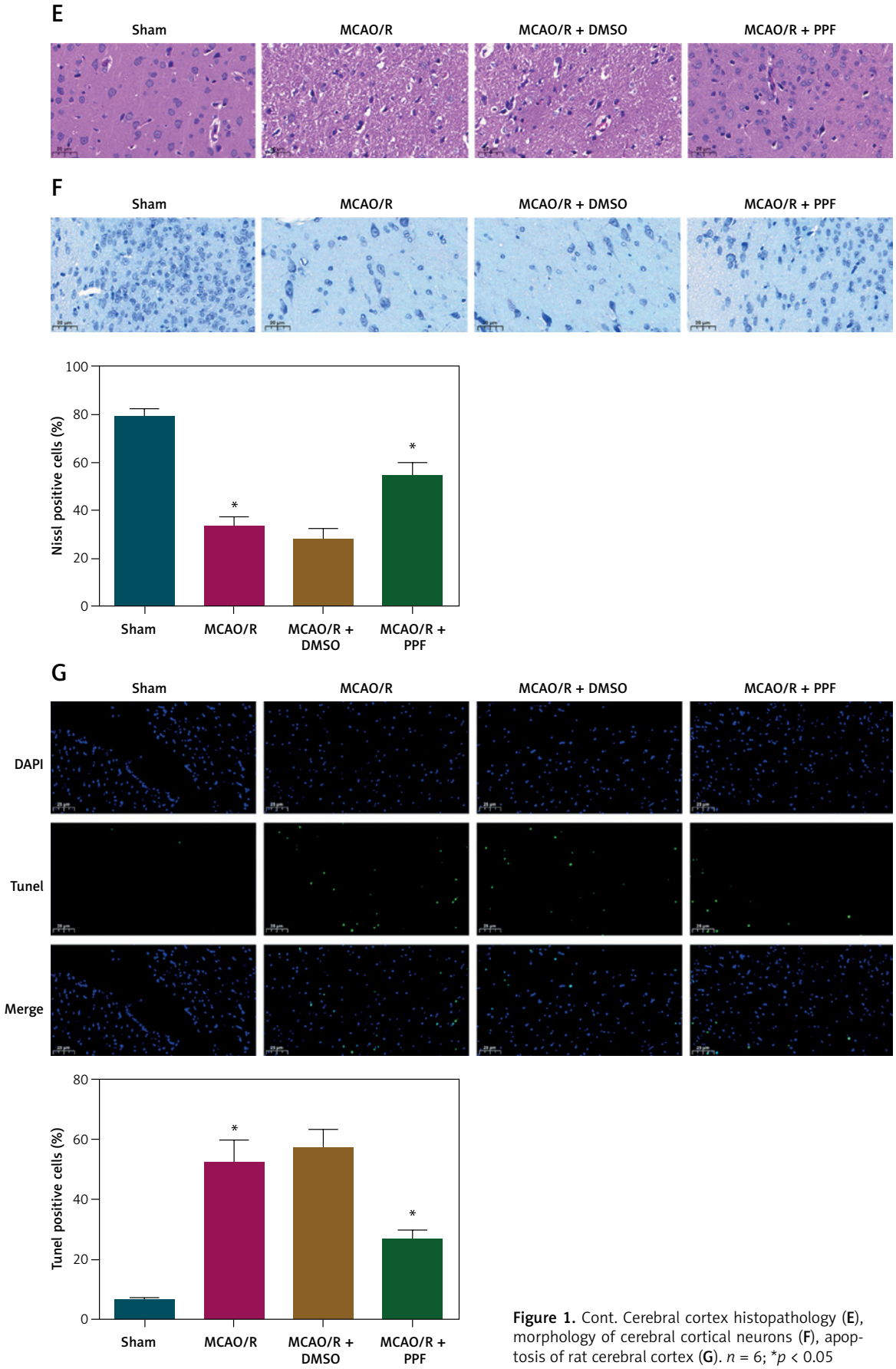

Figure 1. Cont. Cerebral cortex histopathology (**E**), morphology of cerebral cortical neurons (**F**), apoptosis of rat cerebral cortex (**G**). $n = 6$; $^*p < 0.05$

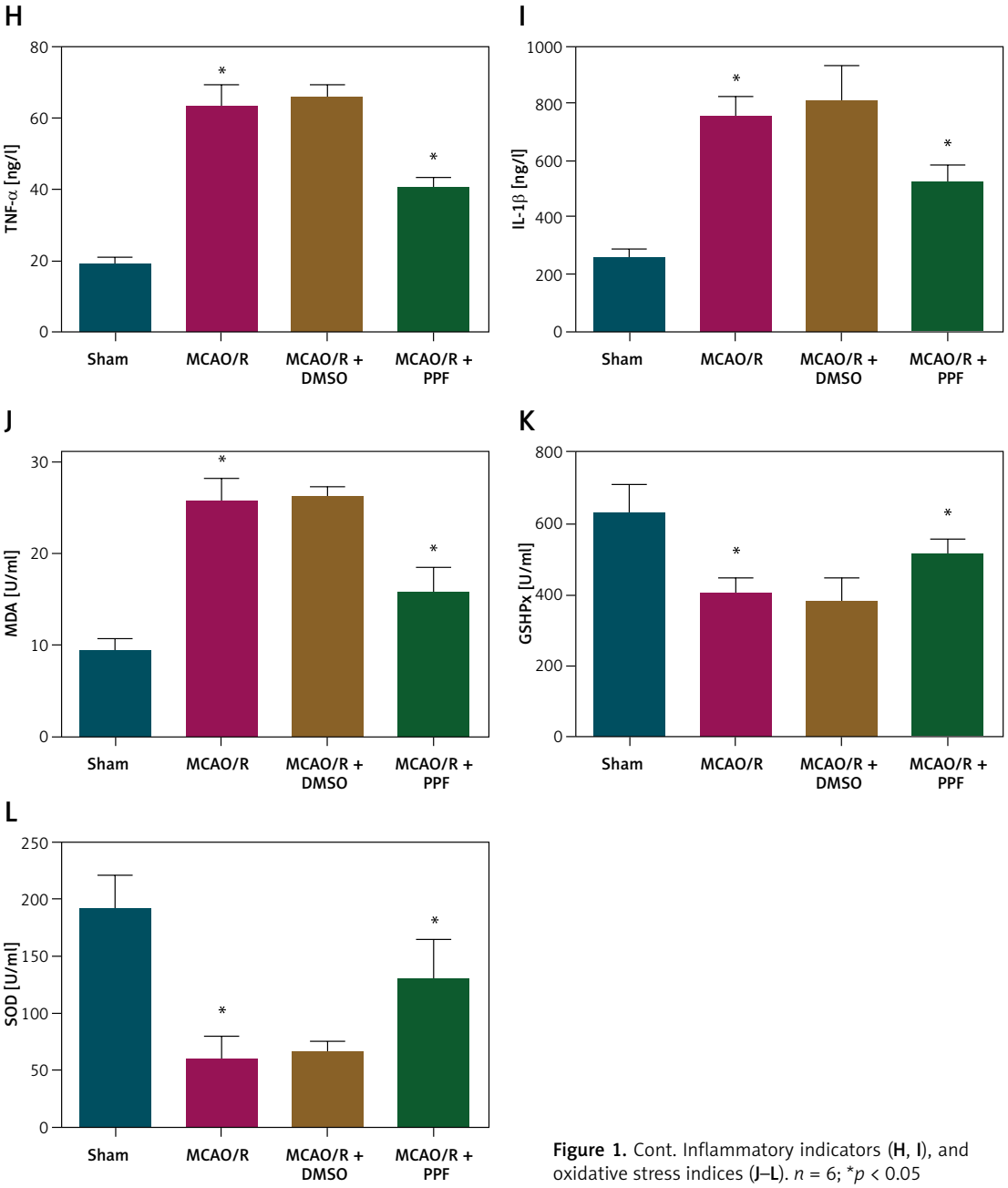

Figure 1. Cont. Inflammatory indicators (**H**, **I**), and oxidative stress indices (**J–L**). $n = 6$; $^*p < 0.05$

Using a microsyringe, 50 µl of lentivirus was slowly injected into the right cerebral cortex of the rats. AgomiR-NC, agomiR-miR-6838-5p, lentiviral vectors for AQP11 (LV-AQP11), and non-targeting plasmid (LV-NC) were obtained from RIBOBIO (Guangzhou, China). From a total of 65 rats, 59 were treated with MCAO/R, and 6 underwent sham operations. The study excluded five rats that died during the MCAO/R treatment and intraperitoneal injection. No mortality was observed in the sham group. Following the modeling, rats were euthanized by cervical dislocation, and brain tissues were extracted.

Neurological deficit score

At 24 h after reperfusion, neurological deficits were evaluated using a standardized scoring system: 0 = no deficit; 1 = failure to fully extend the contralateral forepaw; 2 = incomplete forepaw extension; 3 = mild contralateral rotation; 4 = vigorous contralateral rotation; 5 = falling to the contralateral side. All assessments were conducted by a blinded investigator [31].

Measurement of brain edema

The measurement of cerebral edema was conducted by assessing the water content in the brain. To determine the wet weight (WW), the cerebral

hemispheres were weighed and then dried at 105°C for 24 h to obtain the dry weight (DW). The formula for determining brain water content was: Brain water content = (WW – DW)/WW × 100% [32].

2,3,5-Triphenyl tetrazolium chloride (TTC) staining

Brain tissues were incubated on ice for 24 h, sectioned into continuous coronal slices, and placed in 2% TTC staining solution at 37°C for 20 min. TTC staining was halted by washing with phosphate-buffered saline (PBS), and tissues were fixed in 4% paraformaldehyde for 2 h. Infarcted regions appeared unstained and were quantified as infarct volume relative to total brain volume using Image Pro Plus 6.0 software. Infarct volume (%) was calculated as the total infarct volume divided by the total brain volume, multiplied by 100%.

Hematoxylin and eosin (HE) staining

Rat brain tissues were fixed in 4% paraformaldehyde (Sigma-Aldrich, Merck KGaA), and subsequently hydrated and permeabilized. Tissues were then embedded in paraffin, sectioned into 4 µm slices, and subjected to HE staining. Each slice was examined under a light microscope at 200× magnification in three fields.

Nissl staining

Paraffin-embedded brain sections were dehydrated and stained with cresyl violet solution for 1 h. Following staining, slices were rinsed sequentially with 70%, 80%, and 95% ethanol (10 s each), dehydrated with anhydrous ethanol (5 min per step, twice), cleared with xylene (5 min each step, twice), mounted with neutral gum, and observed under a microscope (Nikon).

Terminal deoxynucleotidyl transferase dUTP nick end labeling (TUNEL) staining

TUNEL staining was performed using a TUNEL kit (Qiming Bio Engineering Co., Ltd., Shanghai, China; OX02752). Sections of rat brain tissue underwent fixation using 4% paraformaldehyde for 20 min, were permeabilized using 0.1% Triton X-100 for 5 min, and then subjected to incubation with a TUNEL reaction blend (in darkness at 37°C for 1.5 h). The samples underwent counterstaining using 4,6-diamidino-2-phenylindole (DAPI). Apoptotic cells testing positive for TUNEL were measured using fluorescence microscopy [33].

Enzyme-linked immunosorbent assay (ELISA)

Rat brain tissues were homogenized in PBS on ice and centrifuged at 3500 rpm for 15 min. The supernatant was collected, and levels of tumor necrosis factor-α (TNF-α; orb79138, Biorbyt) and interleukin-1β (IL-1β; orb79117, Biorbyt) were measured using respective ELISA kits. Absorbance was read at 450 nm using a microplate reader (RT-6100, LeiDu).

Determination of oxidative stress indicators

Malondialdehyde (MDA), glutathione peroxidase (GSH-Px), and superoxide dismutase (SOD) in rat brain tissues and PC12 cells were quantified using specific detection kits (JK-(a)-2197, JK-(a)-2396, JK-(a)-2293; Jingkang Bioengineering Co., Ltd., Shanghai, China).

Cell culture

PC12 cells, sourced from the China Center for Type Culture Collection in Wuhan, China, were grown in Dulbecco's Modified Eagle Medium (DMEM), enriched with 10% fetal bovine serum (Beyotime, Shanghai, China), 100 U/ml penicillin, and 0.1 mg/ml streptomycin (Invitrogen), in an environment at 37°C and 5% CO_2. To create the H/R injury model, PC12 cells were categorized into three distinct groups:

- Control Group: growing in a normoxic environment (21% O_2, 5% CO_2, 74% N_2) devoid of PPF treatment.
- Group H/R: subjected to hypoxia (1% O_2, 5% CO_2, 94% N_2) for 2 h, then reoxygenated in normoxic environments.
- H/R + PPF Group: pre-treated with PPF (50 µM; Sigma-Aldrich) for 1 h prior to H/R injury [34].

Cell viability

PC12 cells (2 × 10^3 cells/well) were seeded into 96-well plates and incubated at 37°C in 5% CO_2 for 72 h. Cell viability was assessed using the 3-(4,5-dimethyl-2-thiazolyl)-2,5-diphenyl-2-H-tetrazolium bromide (MTT) assay kit (Sigma-Aldrich). Briefly, 20 µl of MTT solution was added to each well and incubated at 37°C for 4 h. Subsequently, 150 µl of dimethyl sulfoxide (DMSO; Sigma-Aldrich) was added to dissolve the formazan crystals. Optical density was measured at 570 nm using a Bio-Tek microplate reader (Hopkinton, MA, USA).

Cell apoptosis

The measurement of apoptosis was conducted with the Annexin V-fluorescein isothiocyanate (FITC)/propidium iodide (PI) Apoptosis Detection Kit (Sangon Biotech, Shanghai, China). PC12 cells, totaling 5 × 10^5 cells per well, were cultured in 6-well plates and subjected to a 5-minute incubation with 5 µl of Annexin V-FITC and 10 µl of PI at ambient temperature in darkness. Flow cytometry was performed using a FACS Verse flow cytome-

ter (BD Biosciences), and the data were examined with FlowJo software (version 10; TreeStar) [35].

Quantitative analysis of mRNA expression

RNA was extracted from brain tissues and PC12 cells using Trizol reagent (Invitrogen). For miRNA analysis, cDNA was synthesized using the TaqMan MicroRNA Reverse Transcription Kit (Applied Biosystems) with specific stem-loop RT primers. For mRNA analysis, cDNA was synthesized using the PrimeScript RT kit (Takara). Expression levels of miR-6838-5p and AQP11 were quantified using SYBR Green Real-Time PCR Master Mix (Takara) on a 7500 Real-Time PCR System (Applied Biosystems). The internal control for AQP11 was β-actin, and miR-6838-5p was referenced using U6. Primer sequences are listed in Table I.

Quantitative analysis of protein expression

Proteins were harvested from rat brain mixtures using a radioimmunoprecipitation assay lysis buffer (Beyotime). Protein concentrations were measured with a bicinchoninic acid protein assay kit. The proteins were denatured by boiling, separated using sodium dodecyl sulfate-polyacrylamide gel electrophoresis, and transferred to a polyvinylidene fluoride membrane, which was blocked using 5% skim milk and subjected to overnight incubation at 4°C with primary antibodies targeting AQP11 (1 : 100; ab122821, Abcam), AQP1 (1 : 1000; AB2219, MilliporeSigma), AQP4 (1 : 1000; AB3594, MilliporeSigma), AQP9 (1 : 1000; sc-74409, Santa Cruz Biotechnology), and β-actin (1 : 1000; ab8277, Abcam). The membrane was incubated with a horseradish peroxidase-labeled goat anti-rabbit IgG secondary antibody (1 : 10,000; AB175781, Abcam) at ambient temperature for an 1 h. Protein bands were visualized using an enhanced chemiluminescence agent. Bands intensities were measured with the ImagePro Plus 6.0 software.

Luciferase reporter gene assay

TargetScan software predicted that miR-6838-5p targets AQP11. Wild-type (AQP11-WT) and mutant (AQP11-MUT) fragments containing potential miR-6838-5p binding sites were cloned into the pMIR-REPORT plasmid vector (Promega). The luciferase reporter constructs were co-transfected with miR-6838-5p mimic into PC12 cells using Lipofectamine 2000 reagent (Invitrogen). After 24 h, luciferase activity was measured using a luciferase assay kit (Promega) [36].

RNA immunoprecipitation (RIP) assay

RIP assays were conducted using a RIP kit (Millipore). Cells were lysed with RIP lysis buffer, and the lysate was incubated with RIP buffer containing human anti-AGO2-conjugated magnetic beads. The immunoprecipitated complexes were treated with protease K to digest proteins, and the associated RNA was isolated. The presence of miR-6838-5p and AQP11 in the precipitated RNA was determined by RT-qPCR [37].

Table I. Primers used in PCR

Gene	Sequence (5′→3′)
miR-6838-5p	F:GCACTCCTGGATGCCAATCT
	R:CTCTACAGCTATATTGCCAGCCAC
AQP11	F:GCCTTCGTCCTGGAGTTTCT
	R:GCACCAAGGAAAAGAAGTAGAT
U6	F:CTCGCTTCGGCAGCACA
	R:AACGCTTCACGAATTTGCGT
β-actin	F:GGAGATTACTGCCCTGGCTCCTAGC
	R:GGCCGGACTCATCGTACTCCTGCTT

Note: miR-6838-5p – microRNA-6838-5p; AQP11 – aquaporin11.

Statistical analysis

Data were analyzed using SPSS version 21.0 software. Normality was assessed using the Kolmogorov-Smirnov test. Results are presented as mean ± standard deviation. For comparisons involving multiple groups, one-way analysis of variance followed by the least significant difference post hoc test was used. Categorical data (rates or percentages) were compared using the χ^2 test. All statistical analyses were two-tailed, with a p-value under 0.05 deemed statistically significant.

Results

PPF mitigates oxidative stress injury in MCAO/R rats

To investigate the role of PPF in CI/RI, an MCAO/R rat model was established, and PPF treatment (10 mg/kg) was administered. Previous studies have determined the LD_{50} of PPF in rats to be 22.6 mg/kg, which is significantly higher than the 10 mg/kg used in this study, confirming its safety [38]. Neurological function scores revealed that MCAO/R rats exhibited severe neuronal damage, which was alleviated by PPF treatment (Figure 1 B, $p < 0.05$). Cerebral edema was assessed by measuring brain water content, which was elevated in MCAO/R rats but significantly reduced following PPF administration (Figure 1 C, $p < 0.05$). TTC staining demonstrated substantial infarct areas in MCAO/R rats, whereas PPF treatment resulted in a notable reduction in infarct size (Figure 1 D, $p < 0.05$). HE staining indicated that sham-operated rats had clear and intact tissue structures with dense cell distribution, normal nuclear morphol-

ogy, and no evidence of tissue hydrolase release. In contrast, MCAO/R rats exhibited loose cell arrangement, neuronal degeneration and necrosis, nuclear shrinkage, obscured nucleoli, and large intercellular voids. PPF treatment significantly attenuated cerebral cortical injury in MCAO/R rats (Figure 1 E). Nissl staining revealed severe neuronal loss in MCAO/R rats, which was markedly reduced by PPF treatment (Figure 1 F, $p < 0.05$). TUNEL staining showed a significant increase in apoptotic cells in the cerebral cortex of MCAO/R rats, which was reduced by PPF treatment (Figure 1 G, $p < 0.05$). Inflammatory and oxidative stress markers, which are central to CI/RI pathophysiology, were elevated in MCAO/R rats. PPF intervention resulted in decreased TNF-α, IL-1β, and MDA, while promoting GSH-Px and SOD activities (Figures 1 H–L, $p < 0.05$).

miR-6838-5p enhances anti-inflammatory and antioxidant responses in MCAO/R rats

In the MCAO/R model, the expression of miR-6838-5p was significantly downregulated, as demonstrated by quantitative RT-PCR analysis (Figure 2 A, $p < 0.05$). To investigate the functional

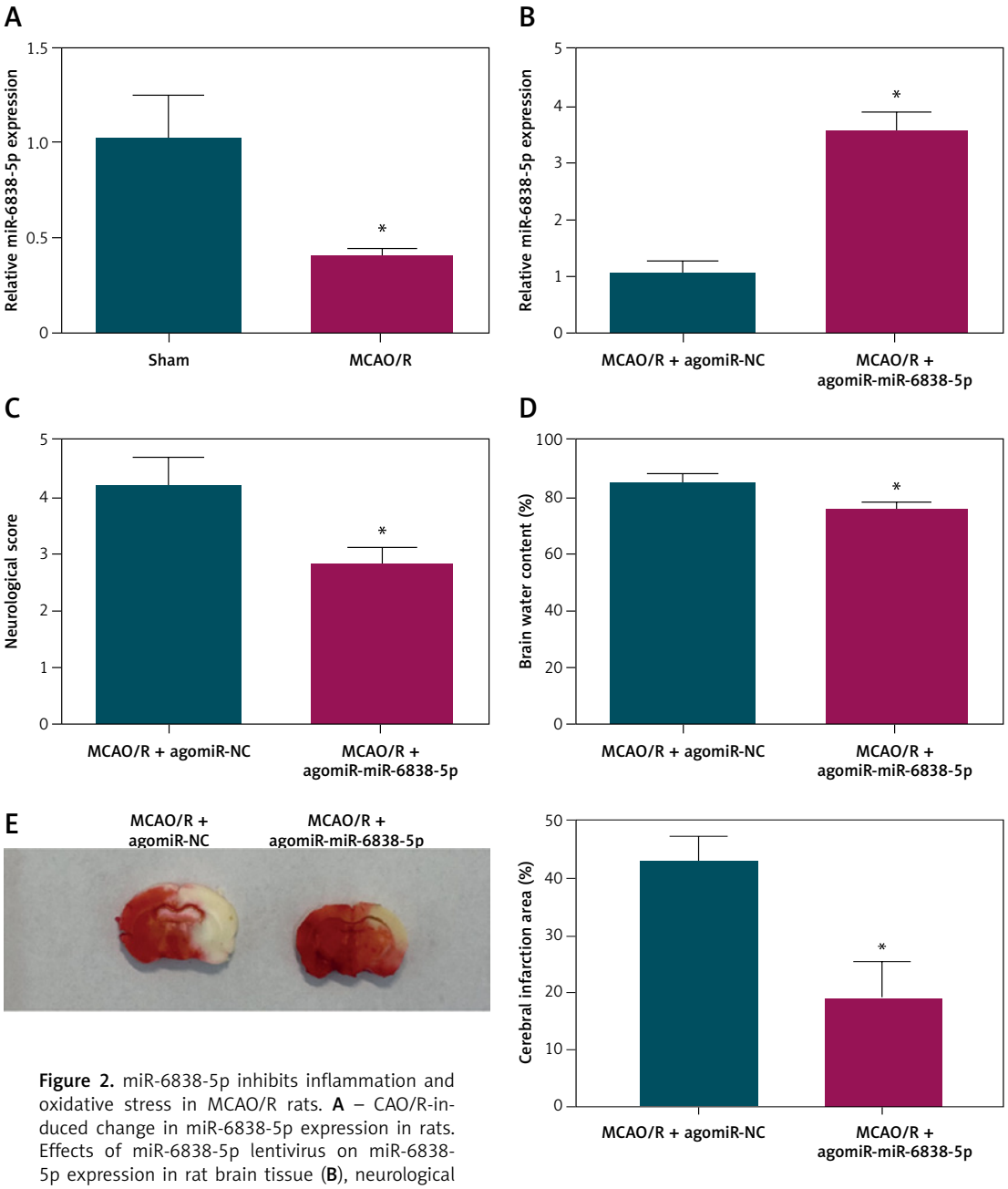

Figure 2. miR-6838-5p inhibits inflammation and oxidative stress in MCAO/R rats. **A** – CAO/R-induced change in miR-6838-5p expression in rats. Effects of miR-6838-5p lentivirus on miR-6838-5p expression in rat brain tissue (**B**), neurological function (**C**), cerebral edema (**D**), infarction area (**E**). $n = 6$; $^*p < 0.05$

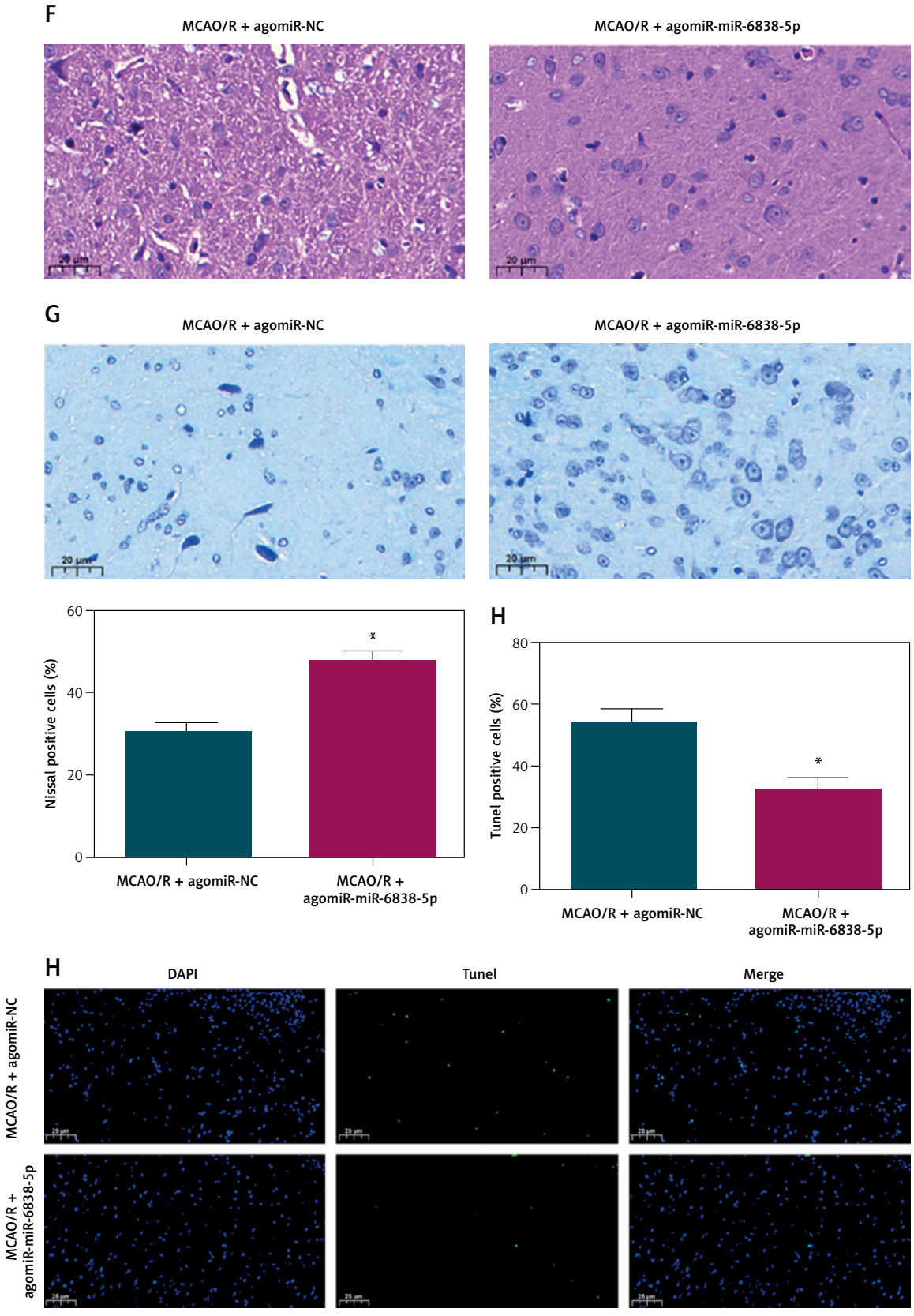

Figure 2. Cont. Cerebral cortex histopathology (**F**), morphology of cerebral cortical neurons (**G**), apoptosis of rat cerebral cortex (**H**). $n = 6$; $^*p < 0.05$

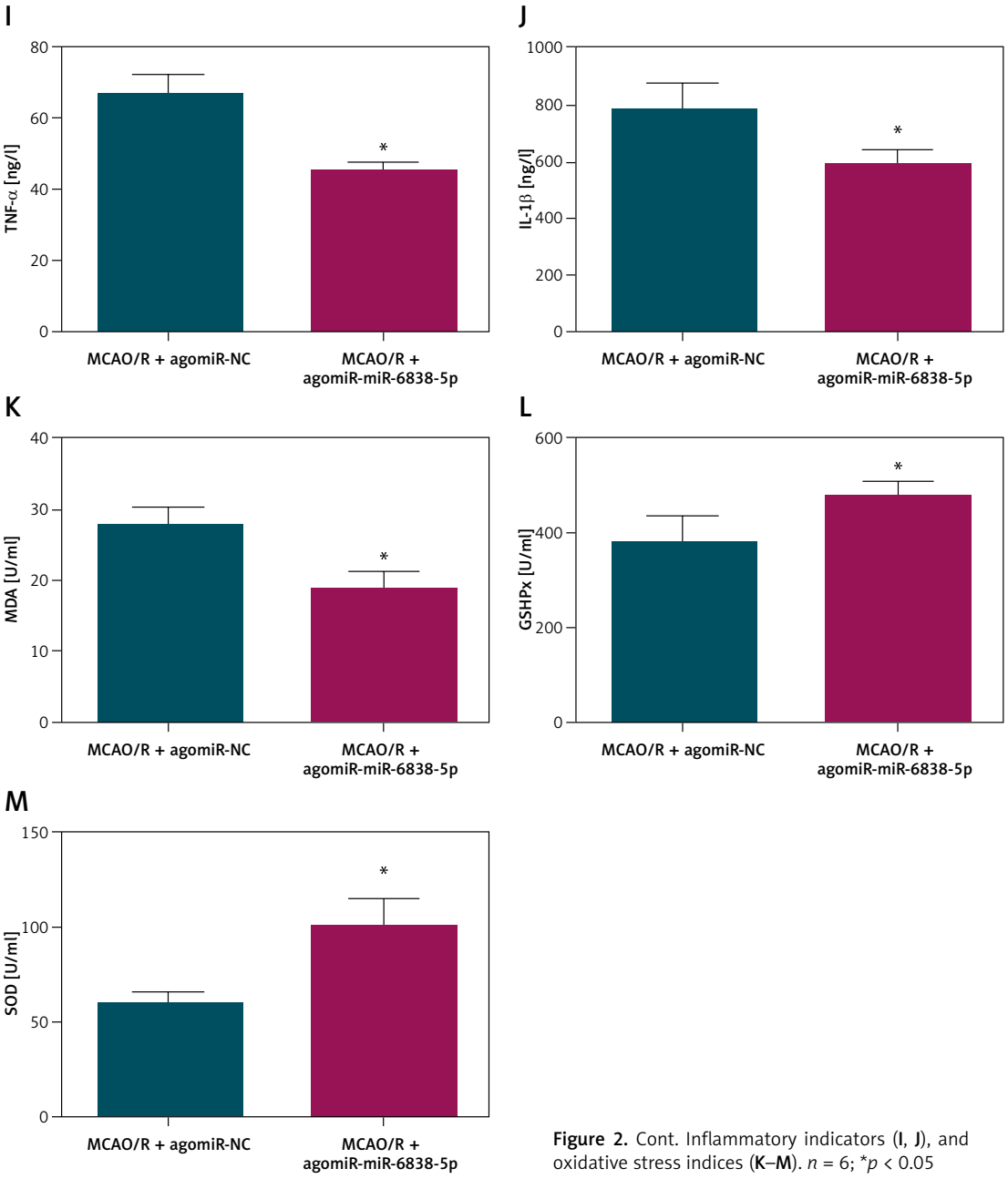

Figure 2. Cont. Inflammatory indicators (**I**, **J**), and oxidative stress indices (**K**–**M**). $n = 6$; *$p < 0.05$

role of miR-6838-5p in this ischemic injury model, we employed lentiviral vectors to overexpress miR-6838-5p in MCAO/R rats prior to the induction of ischemia–reperfusion. Successful overexpression was confirmed by a substantial increase in post-injection miR-6838-5p levels (Figure 2 B, $p < 0.05$). Histological examination revealed that miR-6838-5p overexpression markedly mitigated neuronal damage, as evidenced by reduced neuronal loss and structural preservation in brain tissue sections (Figure 2 C, $p < 0.05$). Additionally, rats with elevated miR-6838-5p exhibited a significant decrease in brain water content, indicating reduced cerebral edema (Figure 2 D, $p < 0.05$), and a notable reduction in infarct size, assessed through infarct volume measurements (Figure 2 E, $p < 0.05$). Further pathological assessment using HE staining demonstrated that miR-6838-5p overexpression led to improved brain tissue morphology, with fewer signs of necrosis and inflammation compared to control groups (Figure 2 F). Apoptotic analysis via TUNEL staining revealed a significant decrease in neuronal apoptosis in the miR-6838-5p overexpressing group (Figures 2 G, H, $p < 0.05$). At the molecular level, overexpression of miR-6838-5p was associated with suppressed inflammatory responses, as indicated by reduced TNF-α and IL-1β (Figures 2 I, J, $p < 0.05$). Concurrently, markers of oxidative stress were ameliorated; MDA levels were significantly decreased (Fig-

ure 2 K, $p < 0.05$), while the activities of GSH-Px and SOD were markedly increased (Figures 2 L, M, $p < 0.05$). Collectively, these results suggest that miR-6838-5p plays a pivotal role in enhancing anti-inflammatory and antioxidant defenses, thereby conferring neuroprotection in MCAO/R-induced ischemic injury.

Inhibition of miR-6838-5p diminishes the therapeutic efficacy of PPF in MCAO/R rats

Treatment with PPF was found to restore the suppressed expression of miR-6838-5p in MCAO/R rats, as evidenced by increased miR-6838-5p levels after PPF administration (Figure 3 A, $p < 0.05$). To delineate the interaction between PPF and miR-6838-5p, a miR-6838-5p antagonist was administered alongside PPF treatment to effectively inhibit miR-6838-5p expression, which was confirmed by RT-qPCR (Figure 3 B, $p < 0.05$). The inhibition of miR-6838-5p significantly abrogated the neuroprotective effects of PPF in MCAO/R rats. Specifically, neuronal injury scores were elevated (Figure 3 C, $p < 0.05$), indicating increased neuronal damage. Additionally, brain water content was significantly higher in the miR-6838-5p-inhibited group, suggesting exacerbated cerebral edema (Figure 3 D,

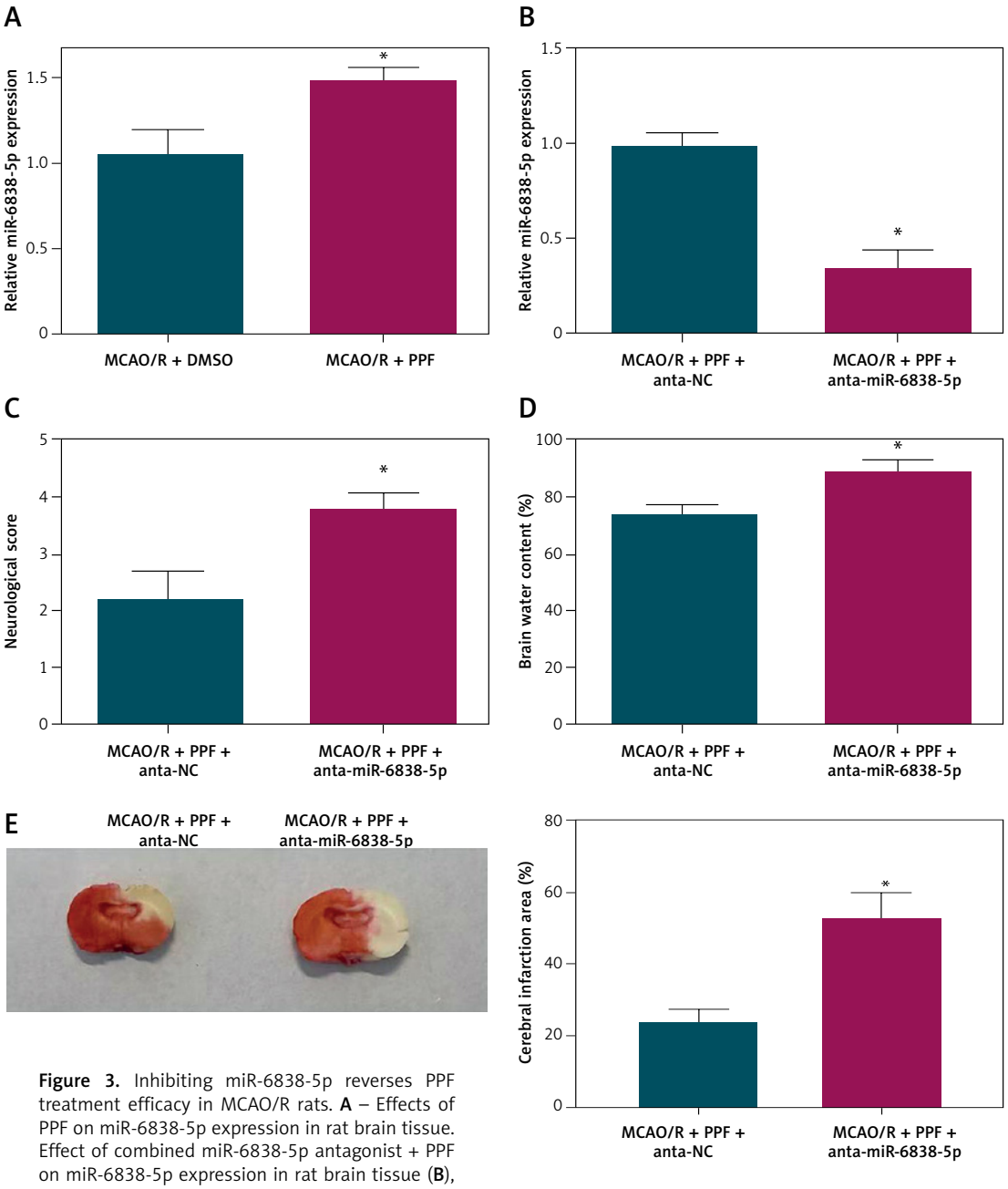

Figure 3. Inhibiting miR-6838-5p reverses PPF treatment efficacy in MCAO/R rats. **A** – Effects of PPF on miR-6838-5p expression in rat brain tissue. Effect of combined miR-6838-5p antagonist + PPF on miR-6838-5p expression in rat brain tissue (**B**), neurological function (**C**), cerebral edema (**D**), infarction area (**E**). $n = 6$; $^*p < 0.05$

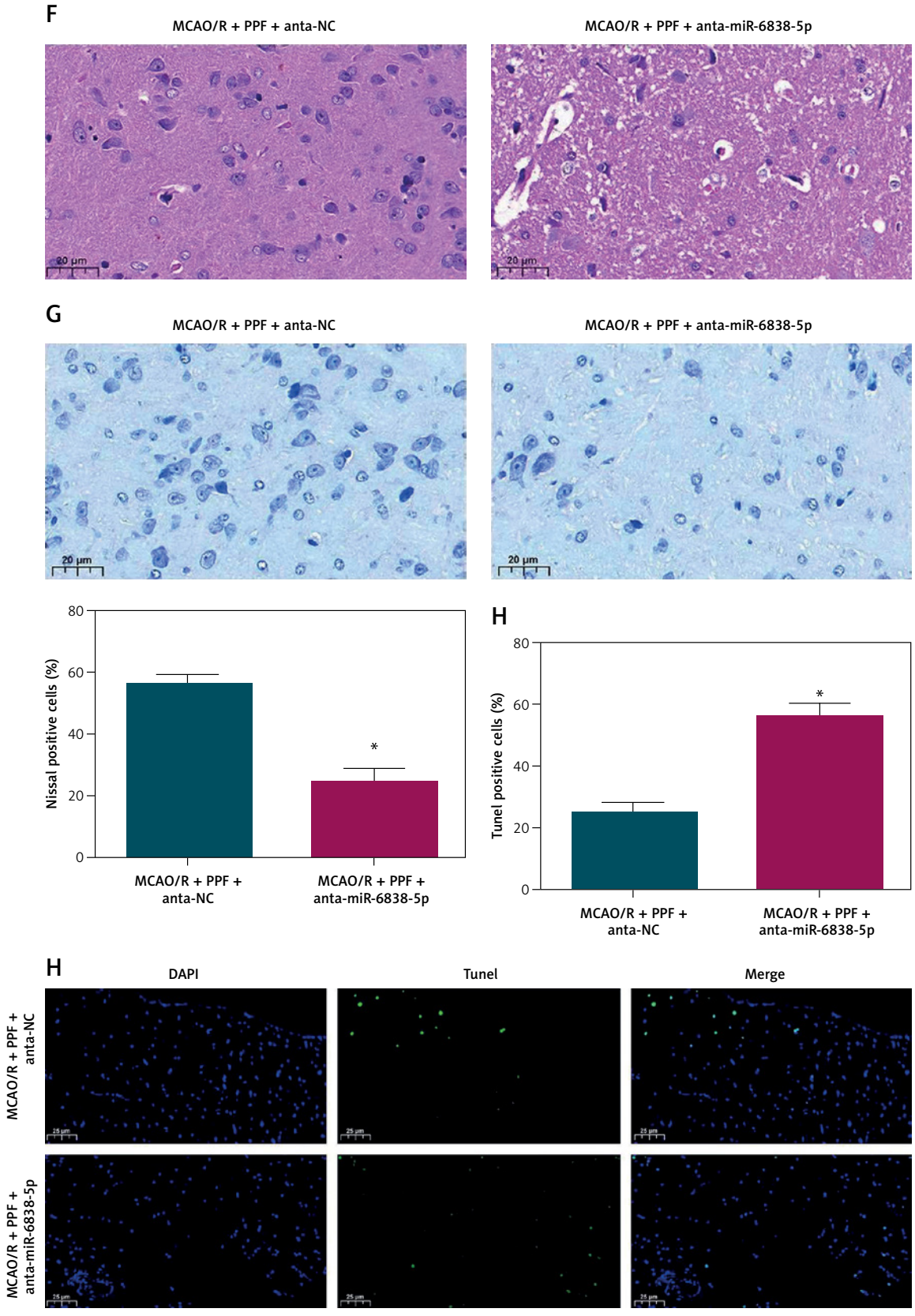

Figure 3. Cont. Cerebral cortex histopathology (**F**), morphology of cerebral cortical neurons (**G**), apoptosis of rat cerebral cortex (**H**). $n = 6$; $^*p < 0.05$

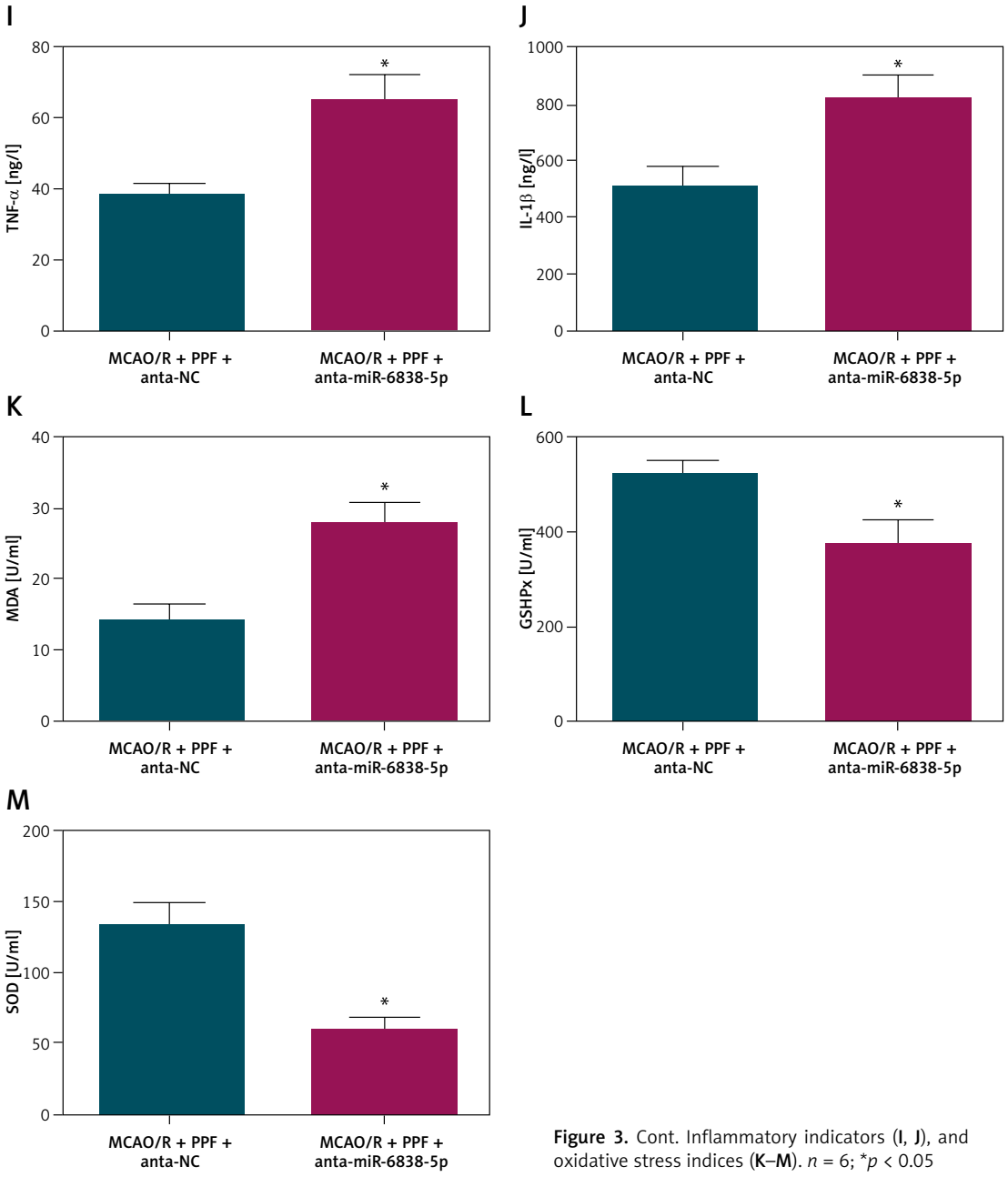

Figure 3. Cont. Inflammatory indicators (**I**, **J**), and oxidative stress indices (**K**–**M**). $n = 6$; *$p < 0.05$

$p < 0.05$). Infarct size measurements revealed an enlargement of the infarct area upon miR-6838-5p inhibition (Figure 3 E, $p < 0.05$). Histopathological analysis using HE staining showed aggravated brain tissue pathology, characterized by increased necrosis and inflammation (Figure 3 F). TUNEL assays further confirmed an increase in neuronal apoptosis in the miR-6838-5p-inhibited group (Figures 3 G, H, $p < 0.05$). At the molecular level, inhibition of miR-6838-5p led to elevated TNF-α and IL-1β (Figures 3 I, J, $p < 0.05$), as well as increased MDA levels (Figure 3 K, $p < 0.05$), indicating heightened oxidative stress. Conversely, the activities of antioxidant enzymes GSH-Px and SOD were significantly suppressed (Figures 3 L, M, $p < 0.05$). These findings collectively demonstrate that miR-6838-5p is indispensable for the therapeutic efficacy of PPF, as its inhibition negates the anti-inflammatory and antioxidant benefits conferred by PPF treatment in MCAO/R-induced ischemic injury.

miR-6838-5p regulates AQP11 expression

We identified potential downstream targets using bioinformatics prediction tools (Figure 4 A). AQP11 emerged as a promising candidate target of miR-6838-5p. Dual luciferase reporter assays were conducted to validate this interaction. The results demonstrated that miR-6838-5p mimics significantly inhibited the luciferase activity of the

AQP11-WT but had no effect on the AQP11-MUT, confirming a direct binding interaction between miR-6838-5p and the 3′ UTR of AQP11 mRNA (Figure 4 B, $p < 0.05$). Further validation was performed using RIP assays, which revealed that miR-6838-5p was significantly enriched in complexes containing AQP11, thereby corroborating the direct interaction between the two molecules (Figure 4 C, $p < 0.05$). Subsequent analysis of protein expression levels in brain tissues of MCAO/R rats

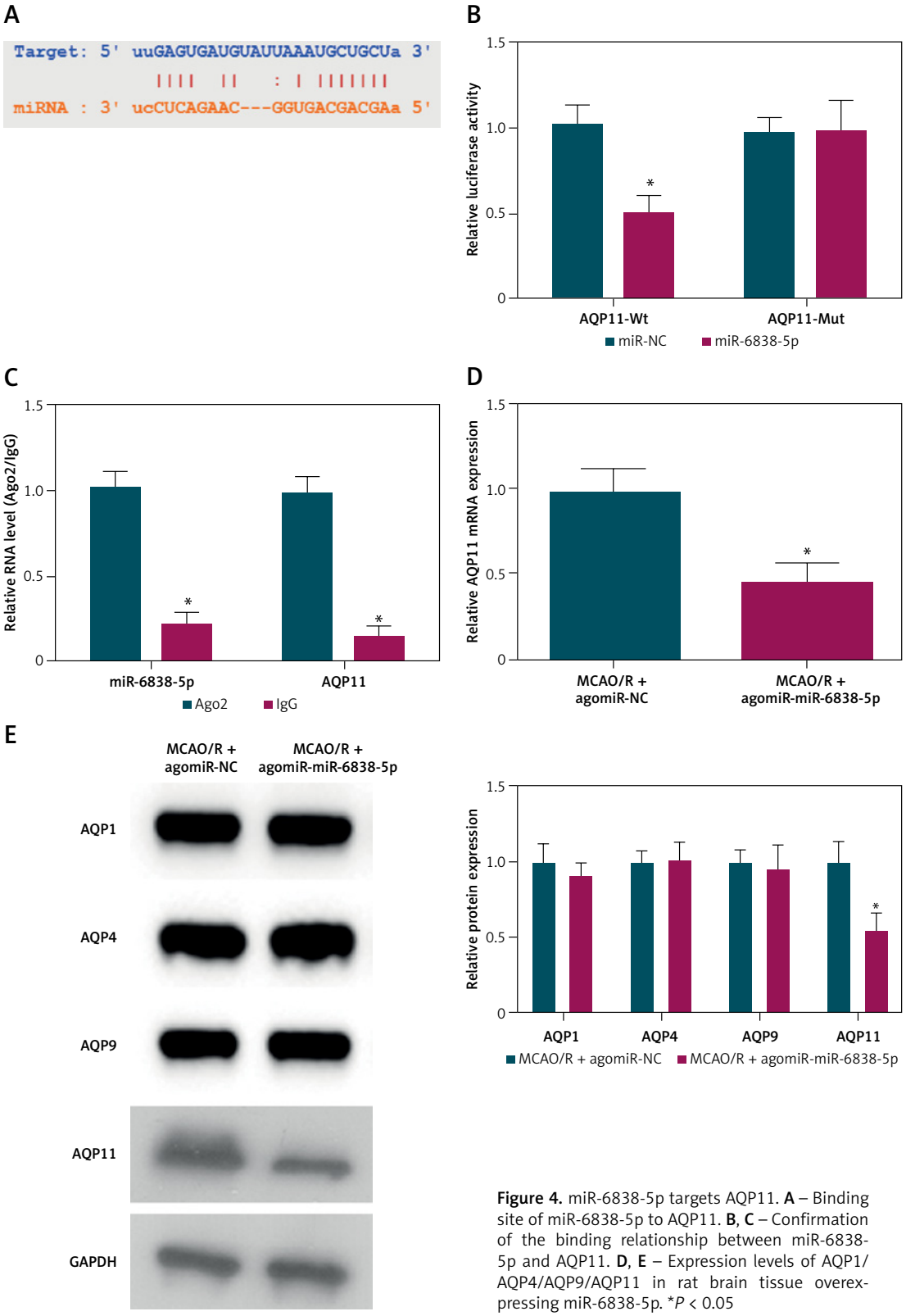

Figure 4. miR-6838-5p targets AQP11. **A** – Binding site of miR-6838-5p to AQP11. **B**, **C** – Confirmation of the binding relationship between miR-6838-5p and AQP11. **D**, **E** – Expression levels of AQP1/AQP4/AQP9/AQP11 in rat brain tissue overexpressing miR-6838-5p. *$P < 0.05$

overexpressing miR-6838-5p showed a significant reduction in AQP11 expression (Figure 4 D, $p < 0.05$). Importantly, the expression levels of other aquaporin family members, including AQP1, AQP4, and AQP9, remained unchanged, indicating the specificity of miR-6838-5p in targeting AQP11 (Figure 4 E, $p < 0.05$). These results collectively establish AQP11 as a direct and specific target of miR-6838-5p, suggesting that the regulatory axis miR-6838-5p/AQP11 plays a crucial role in mediating the anti-inflammatory and antioxidant responses in ischemic injury.

Overexpression of AQP11 impairs the therapeutic effects of PPF in MCAO/R rats

In the MCAO/R rat model, both AQP11 and AQP4 expression levels were significantly elevated, as determined by RT-qPCR and Western blot analyses (Figures 5 A, B, $p < 0.05$). PPF treatment effectively reduced the expression of these aquaporins, suggesting a modulatory effect of PPF on their expression. To further investigate the specific role of AQP11 in mediating the therapeutic effects of PPF, AQP11 was overexpressed in MCAO/R rats prior to administering PPF, which was confirmed by RT-qPCR and Western blot (Figure 5 C, $p < 0.05$). Overexpression of AQP11 in MCAO/R rats undergoing PPF treatment resulted in a significant increase in neuronal injury scores, indicating exacerbated neuronal damage despite PPF administration (Figure 5 D, $p < 0.05$). Additionally, brain water content was markedly elevated in the AQP11-overexpressing group (Figure 5 E, $p < 0.05$), suggesting aggravated cerebral edema. Infarct size measurements revealed that AQP11 overexpression led to significantly larger infarct areas in PPF-treated MCAO/R rats (Figure 5 F, $p < 0.05$). Histopathological analysis using HE staining showed that AQP11 overexpression aggravated brain tissue damage, characterized by increased necrosis and inflammatory cell infiltration (Figure 5 G). TUNEL assays confirmed a significant increase in neuronal apoptosis in the AQP11-overexpressing group (Figures 5 H, I, $p < 0.05$). Elevating AQP11 elevated TNF-α and IL-1β (Figures 5 J, K, $p < 0.05$), as well as increasing MDA levels (Figure 5 L, $p < 0.05$). Concurrently, the activities of GSH-Px and SOD were significantly re-

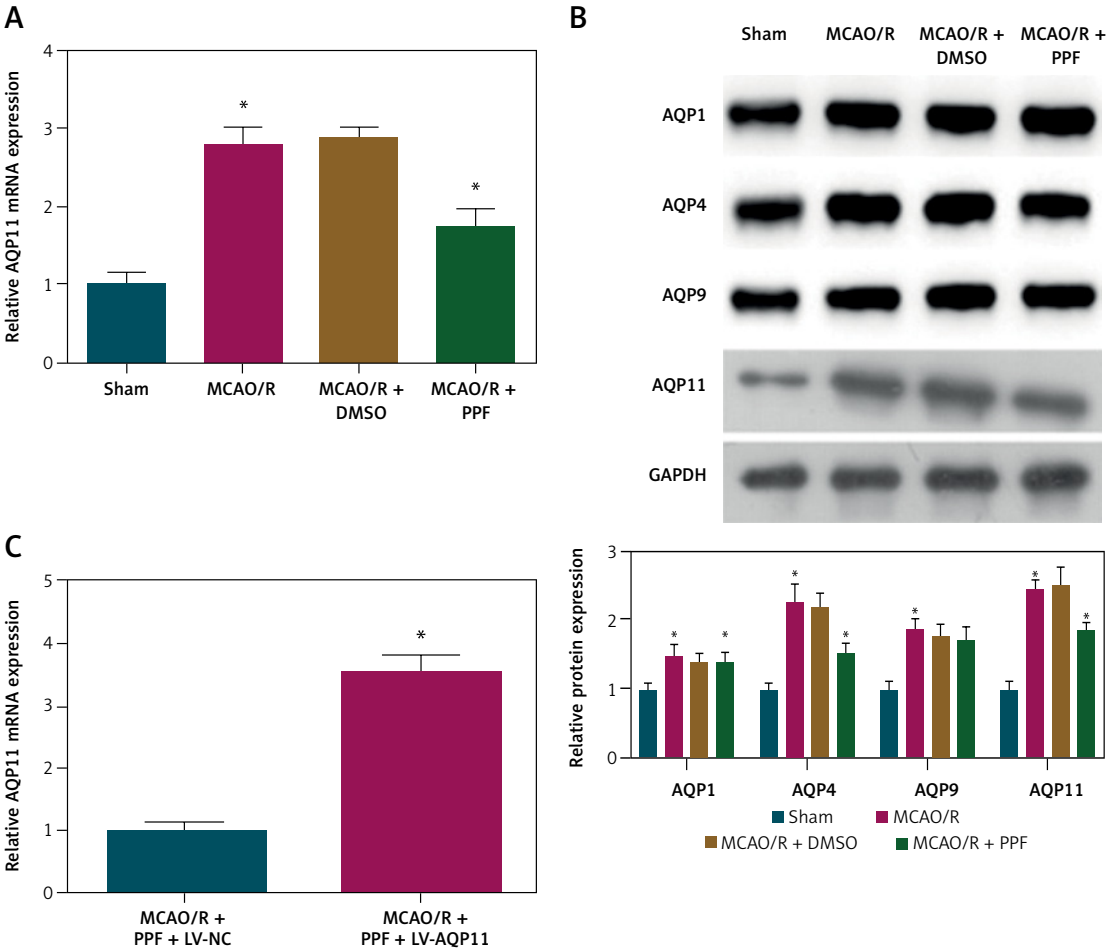

Figure 5. Overexpression of AQP11 reduces the therapeutic effect of PPF on MCAO/R rats. **A**, **B** – MCAO/R-induced change in AQP11 and AQP4 expression in rat brain tissue and effect of PPF on AQP11 and AQP4 expression in MCAO/R rats. Effect of combined lV-AQP11 + PPF on AQP11 expression in rat brain tissue (**C**). $n = 6$; $^*P < 0.05$

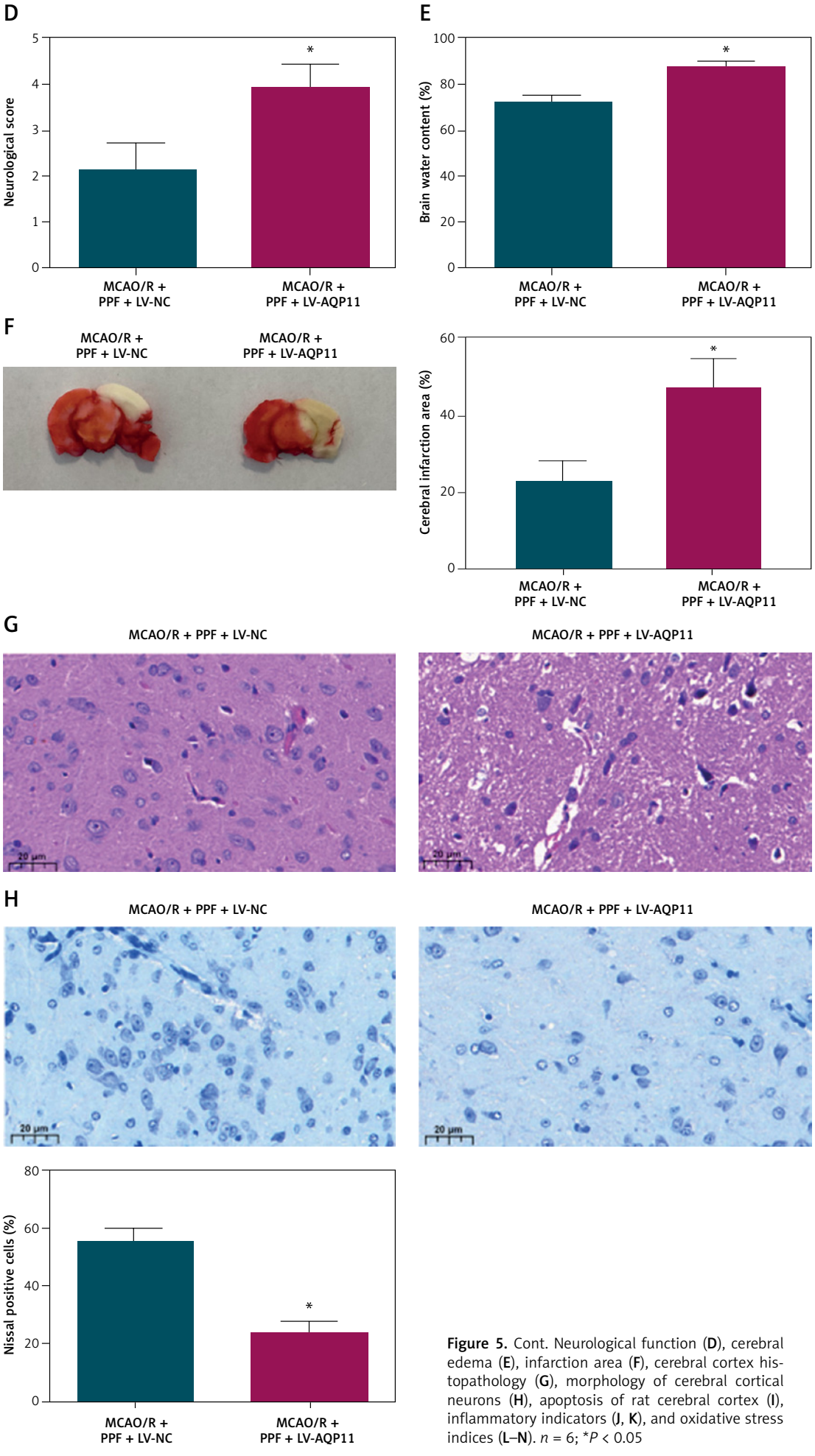

Figure 5. Cont. Neurological function (**D**), cerebral edema (**E**), infarction area (**F**), cerebral cortex histopathology (**G**), morphology of cerebral cortical neurons (**H**), apoptosis of rat cerebral cortex (**I**), inflammatory indicators (**J**, **K**), and oxidative stress indices (**L**–**N**). $n = 6$; $^*P < 0.05$

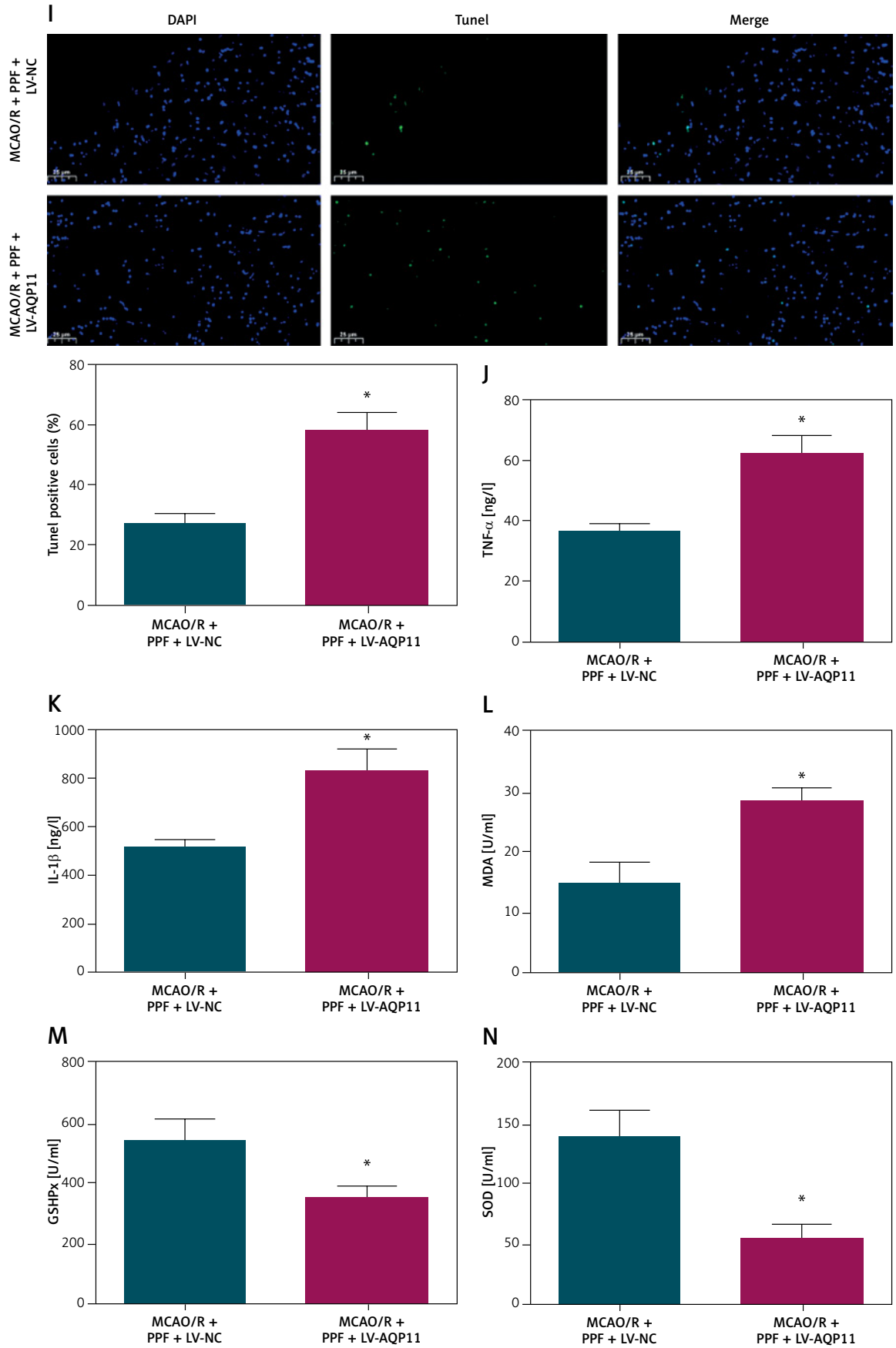

Figure 5. Cont. Apoptosis of rat cerebral cortex (**I**), inflammatory indicators (**J**, **K**), and oxidative stress indices (**L**–**N**). $n = 6$; $^*P < 0.05$

duced (Figures 5 M, N, $p < 0.05$). These findings demonstrate that elevating AQP11 undermines the neuroprotective effects of PPF, thereby highlighting the critical role of the miR-6838-5p/AQP11 axis in mediating the therapeutic actions of PPF in MCAO/R-induced ischemic injury.

PPF alleviates H/R injury in PC12 cells via the miR-6838-5p/AQP11 axis

To translate our *in vivo* findings to an *in vitro* context, we used a PC12 cell model subjected to H/R injury. In this model, miR-6838-5p expression was markedly decreased, while AQP11 expression was significantly increased, mirroring the *in vivo* MCAO/R findings (Figures 6 A–C, $p < 0.05$). Pretreatment with PPF effectively reversed these expression changes, resulting in elevated miR-6838-5p levels and reduced AQP11 expression (Figures 6 A–C, $p < 0.05$), suggesting that PPF modulates the miR-6838-5p/AQP11 axis *in vitro*. Functional assays further elucidated the protective effects of PPF in PC12 cells subjected to H/R injury. The MTT assay revealed that H/R significantly reduced cell viability (Figure 6 D, $p < 0.05$), whereas PPF treatment substantially enhanced cell viability, approaching baseline levels. Flow cytometry analysis demonstrated that H/R induced a significant increase in apoptotic cells (Figure 6 E, $p < 0.05$), which was effectively mitigated by PPF treatment, indicating its anti-apoptotic properties. Moreover, oxidative stress markers were assessed to evaluate the antioxidant effects of PPF. H/R resulted in a significant increase in MDA levels and a concomitant decrease in the activities of GSH-Px and SOD in PC12 cells (Figures 6 F–H, $p < 0.05$). PPF treatment effectively reversed these

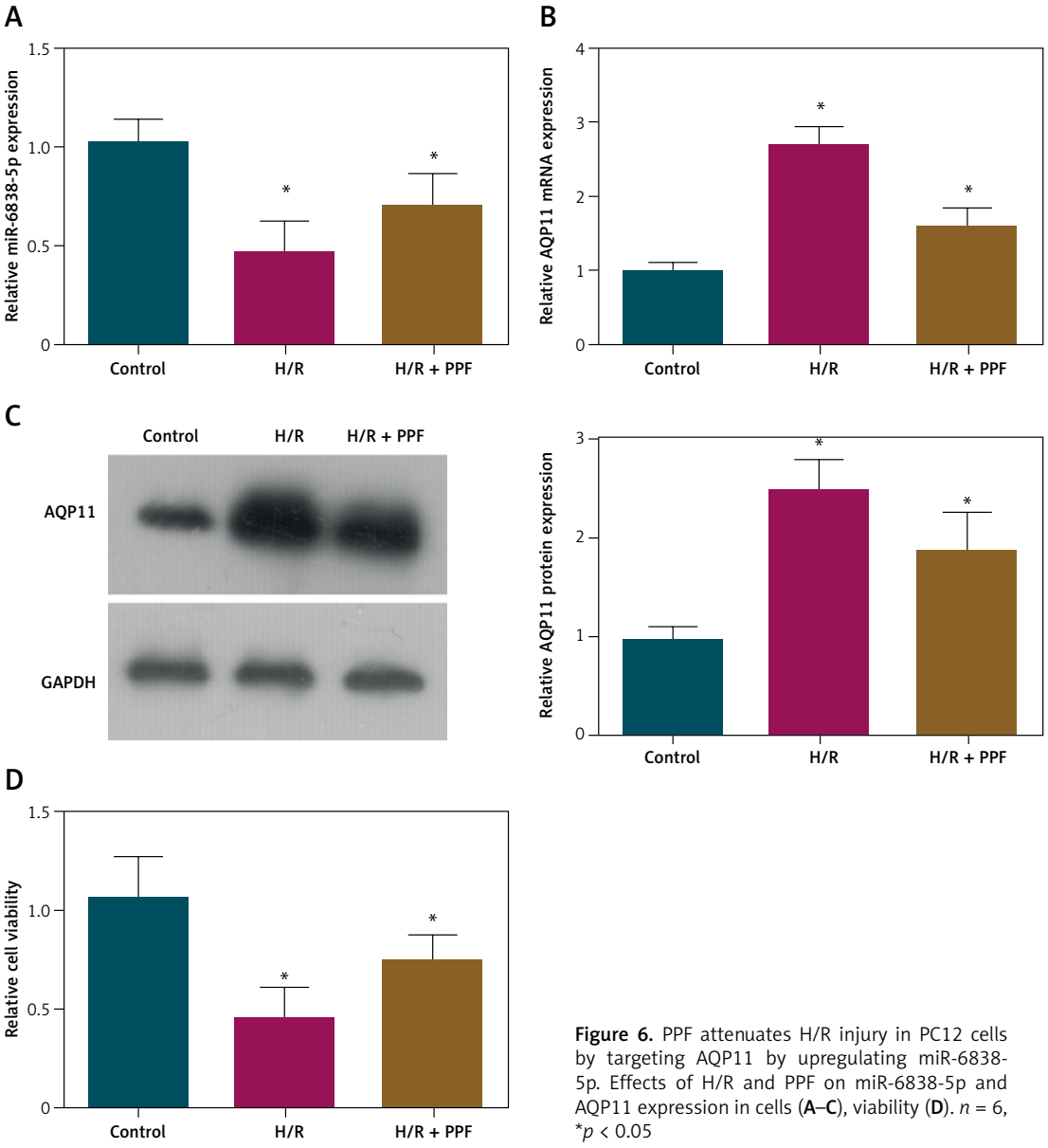

Figure 6. PPF attenuates H/R injury in PC12 cells by targeting AQP11 by upregulating miR-6838-5p. Effects of H/R and PPF on miR-6838-5p and AQP11 expression in cells (**A**–**C**), viability (**D**). $n = 6$, $^*p < 0.05$

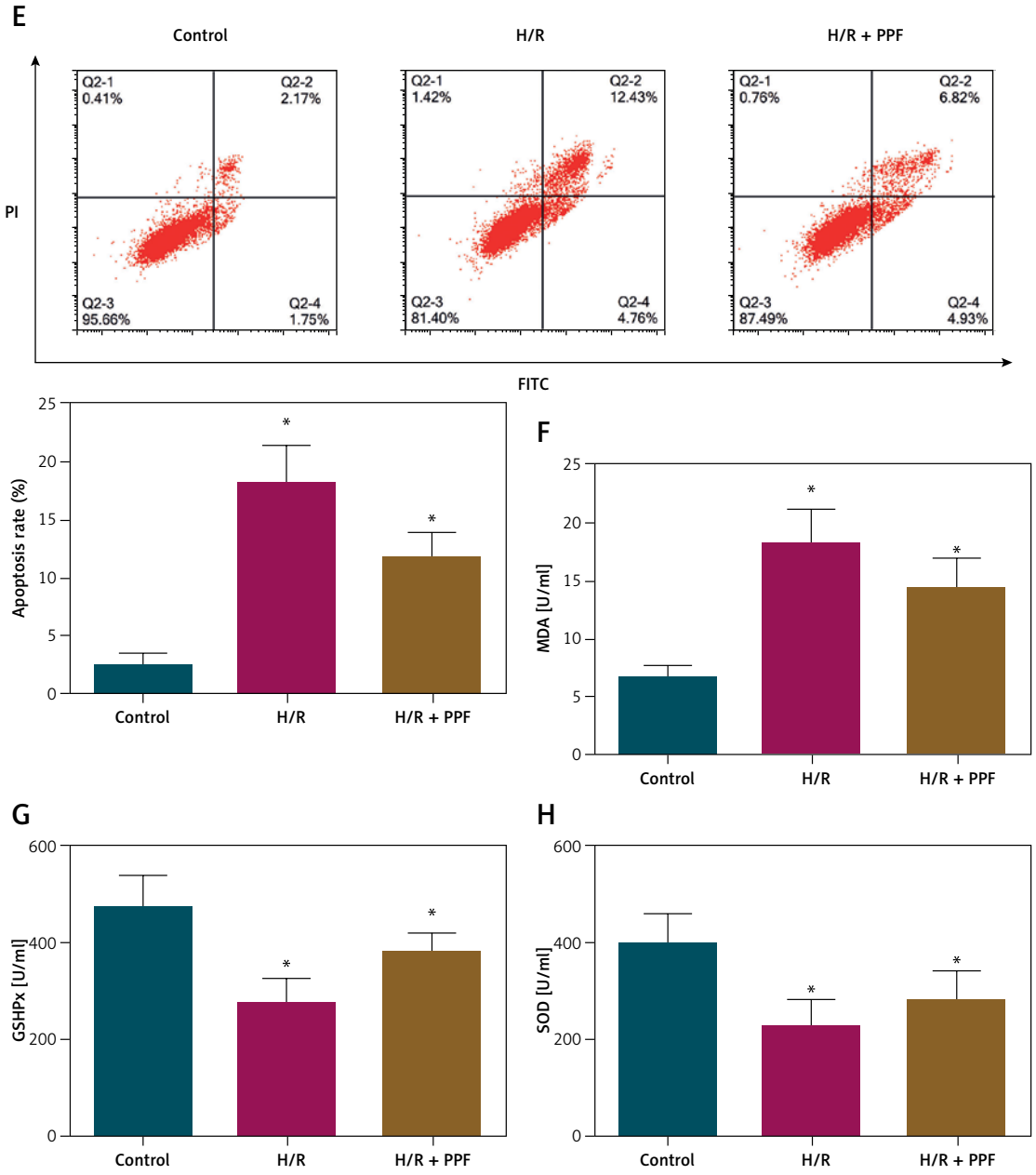

Figure 6. Cont. Apoptosis (**E**), and oxidative stress indicators (**F–H**). $n = 6$, $^*p < 0.05$

alterations by reducing MDA levels and restoring GSH-Px and SOD activities. These *in vitro* results corroborate the *in vivo* data, demonstrating that PPF alleviates H/R-induced cellular injury through the modulation of the miR-6838-5p/AQP11 axis, thereby exerting anti-inflammatory and antioxidant effects.

Discussion

CI/RI poses a significant clinical challenge in the treatment of ischemic stroke [39]. Developing therapeutic agents to alleviate CI/RI is a primary focus in the management of cerebral ischemia. Recent studies have highlighted the potential of PPF as a therapeutic agent for CI/RI. However, the downstream molecular mechanisms mediating its protective effects require further elucidation. This study investigated the protective mechanism of PPF in CI/RI, focusing on the miR-6838-5p/AQP11 axis.

Ischemia-reperfusion injury induces a cascade of physiological and pathological changes, including inflammation, oxidative stress, neuronal apoptosis, and structural brain damage [40, 41]. Our study demonstrated that PPF treatment in MCAO/R rats and H/R-injured PC12 cells resulted in decreased neuronal injury scores, reduced brain water content, improved brain histopathology, decreased neuronal apoptosis, and attenuated oxidative stress and inflammatory responses. These

findings indicate that PPF effectively promotes the repair of CI/RI and the recovery of neurological function.

MiRNAs are extensively found in eukaryotic organisms and are essential for controlling gene expression in biological processes. [42]. Numerous studies have identified the involvement of miRNAs in CI/RI pathophysiology, including miR-374 [43] and miR-219a-5p [44]. Consequently, miRNAs are considered important therapeutic targets in CI/RI progression. Recently, miR-6838-5p has emerged as a miRNA associated with cardiovascular diseases, implicated in the pathogenesis of cerebral hemorrhage injury [39] and myocardial ischemia–reperfusion injury [45, 46]. Notably, our study observed downregulation of miR-6838-5p during MCAO/R modeling. Lentiviral overexpression of miR-6838-5p prior to MCAO/R surgery mitigated inflammation and oxidative stress in MCAO/R rats. miR-6838-5p expression was restored in MCAO/R rats following PPF treatment, hinting at a regulatory relationship between PPF and miR-6838-5p. Functional rescue experiments confirmed that PPF ameliorates pathological damage in MCAO/R rats by upregulating miR-6838-5p.

miRNAs regulate target gene expression by binding to the 3′ UTR of mRNAs [47]. To shed more light on the involvement of miR-6838-5p in CI/RI, we identified AQP11 as a direct target. AQP11 is an intracellular aquaporin that is expressed in multiple tissues, including the brain [48]. miRNA-mediated regulation of AQP11 safeguards against the disruption of the blood-brain barrier and brain injury after intracerebral hemorrhage [49]. In our study, overexpression of AQP11 in MCAO/R rats exacerbated pathological damage, including increased neuronal injury scores, elevated cerebral water content, aggravated brain histopathology, heightened neuronal apoptosis, and enhanced inflammatory and oxidative stress responses.

Therapeutic interventions often exert their effects through downstream molecular pathways. For instance, sevoflurane modulates CI/RI pathophysiology by targeting homeodomain-interacting protein kinase 1 through upregulation of miR-30c-5p [50], while melatonin targets the miR-26a-5p-neuron restrictive silencer factor pathway to enhance autophagy, control inflammation, and lessen oxidative stress in CI/RI. Our study similarly observed that AQP11 expression increased in MCAO/R rats and was significantly lowered with PPF treatment. These findings imply that PPF's protective effect on CI/RI is mediated by miR-6838's regulation of AQP11. Specifically, PPF enhances miR-6838-5p expression, which in turn downregulates AQP11, leading to reduced pro-inflammatory factors and oxidative stress indicators, thereby mitigating pathological injury in MCAO/R rats. Additionally, PPF attenuates H/R injury in PC12 cells by targeting AQP11 through the upregulation of miR-6838-5p, further supporting the *in vivo* findings. Furthermore, PPF may influence upstream regulators of miR-6838-5p, thereby providing a broader understanding of its neuroprotective mechanisms. For example, miR-6838-5p has been found to be targeted for adsorption by a circRNA called circRBM33 in CI/RI [24]. In addition to circRNAs, lncRNAs may also be upstream targets of PPF regulation. In cancer, lncRNA CERS6-AS1 and lncRNA SH3BP5-AS1 have been shown to target adsorption of miR-6838-5p [51, 52]. Therefore, it is necessary to further explore the PPF-influenced circRNAs and lncRNAs by sequencing technology in future studies to further confirm the upstream genes of miR-6838-5p. While our study focused on the downstream effects involving miR-6838-5p and AQP11, it is plausible that PPF interacts with key transcription factors such as NF-κB and Nrf2, or epigenetic regulators such as histone modifying enzymes, to indirectly regulate the expression of miR-6838-5p. Identifying these upstream regulators remains a crucial area for future research, which could be pursued through techniques such as chromatin immunoprecipitation and RNA sequencing to map the regulatory networks influenced by PPF.

Despite confirming the protective effects and underlying mechanisms of PPF against CI/RI, this study has certain limitations. Firstly, upstream regulatory molecules of miR-6838-5p were not explored, which could provide a more comprehensive understanding of the protective mechanisms of PPF in CI/RI. Secondly, potential anti-endoplasmic reticulum stress and other protective effects of PPF were not investigated, which could further elucidate the pharmacological profile of PPF. Moreover, the clinical significance of PPF in CI/RI remains to be evaluated. Currently, the application of PPF for CI/RI treatment is limited to *in vitro* and animal studies, and its clinical use faces significant challenges. The molecular mechanisms by which PPF ameliorates CI/RI are not fully defined, and the appropriate dosing and toxicity of PPF in humans require further investigation. Notably, PPF infusion syndrome (PRIS), a potentially fatal condition, underscores the need to explore PPF toxicity [53]. Future research should focus on delineating the molecular mechanisms of PPF in CI/RI, assessing its toxicity, and identifying agents that can mitigate PRIS. Additionally, combination therapies involving PPF and other drugs may offer a promising approach for effective CI/RI treatment. Furthermore, future studies should explore the role of PPF in other models of neuroprotection and assess the combined effects of multiple therapeutic strategies to enhance treatment efficacy.

Combination therapies involving PPF and other drugs may offer a promising approach for effective CI/RI treatment.

The potential risks associated with targeting miR-6838-5p must be carefully considered, given that miRNAs are widely expressed across multiple tissues. Targeting miR-6838-5p may have unintended off-target effects, potentially affecting the function of other organs such as the heart, liver, and kidneys. Future studies should employ tissue-specific knockdown or overexpression models to evaluate the safety and specificity of miR-6838-5p modulation. Additionally, exploring delivery methods that ensure brain-specific targeting, such as brain-targeted vectors or localized administration, could minimize systemic side effects and enhance therapeutic efficacy. Understanding these aspects is crucial for the safe and effective clinical translation of therapies targeting the miR-6838-5p/AQP11 axis.

This study aligns with previous research on the neuroprotective mechanisms of other anesthetic agents, such as sevoflurane and melatonin, which also modulate specific miRNA axes to exert their protective effects. However, our study is the first to elucidate the role of the miR-6838-5p/AQP11 axis in PPF-mediated neuroprotection in CI/RI, thereby highlighting a novel therapeutic pathway that could be targeted in future interventions. This novel insight provides a solid foundation for therapeutic strategies targeting the miR-6838-5p/AQP11 axis, potentially enhancing the clinical management of ischemic stroke and reducing the associated neurological damage.

Moreover, the study's comprehensive experimental framework, which includes both *in vivo* and *in vitro* models, strengthens the validity of the results and supports the translational potential of targeting the miR-6838-5p/AQP11 axis. Future studies should strive to confirm these findings in clinical trials and assess the broader implications of targeting this axis in other tissues, taking into account the widespread expression of miRNAs and possible off-target effects. Additionally, investigating the long-term effects of miR-6838-5p modulation and PPF treatment on neuronal function and behavioral outcomes will be essential for understanding the sustained impact and safety of such therapeutic interventions.

In conclusion, PPF attenuates oxidative stress injury and inflammation in MCAO/R rats and H/R-injured PC12 cells by targeting AQP11 through the upregulation of miR-6838-5p. This study is the first to elucidate the role of the PPF/miR-6838-5p/AQP11 axis in cerebral ischemia–reperfusion injury, providing novel targets for drug development and therapeutic strategies for CI/RI following ischemic stroke. Future studies should validate these findings through clinical trials, employing multicenter approaches to enhance the generalizability and reproducibility of the results. Additionally, randomized controlled trials should compare the efficacy of PPF with existing treatments, optimize dosing regimens, and assess the safety profile of PPF in human populations. Evaluating the impact of PPF on the clinical prognosis of patients with CI/RI is also essential to translate these preclinical findings into effective clinical interventions. Furthermore, exploring the potential synergistic effects of PPF with other therapeutic agents targeting different molecular pathways may offer more comprehensive neuroprotection and improved clinical outcomes.

Funding

This study was supported by the Shandong Province Traditional Chinese Medicine Science and Technology Project (2021Z009).

Ethical approval

The animal experiment research protocol was approved by the Ethics Committee of our Hospital (SDTHEC) and performed in accordance with the "Guidelines for the care and use of experimental animals".

Conflict of interest

The authors declare no conflict of interest.

References

1. Benjamin EJ, Blaha MJ, Chiuve SE, et al. Heart Disease and Stroke Statistics-2017 Update: a report from the American Heart Association. Circulation 2017; 135: e146-603.
2. Lo WL, Mao YR, Li L, et al. Prospective clinical study of rehabilitation interventions with multisensory interactive training in patients with cerebral infarction: study protocol for a randomised controlled trial. Trials 2017; 18: 173.
3. Feske SK. Ischemic stroke. Am J Med 2021; 134: 1457-64.
4. Obadia N, Lessa MA, Daliry A, et al. Cerebral microvascular dysfunction in metabolic syndrome is exacerbated by ischemia-reperfusion injury. BMC Neurosci 2017; 18: 67.
5. Xue X, Wang H, Su J. Inhibition of MiR-122 decreases cerebral ischemia-reperfusion injury by upregulating DJ-1-phosphatase and tensin homologue deleted on chromosome 10 (PTEN)/phosphonosinol-3 kinase (PI3K)/AKT. Med Sci Monit 2020; 26: e915825.
6. Zhou X, Wang Z, Xu B, et al. Long non-coding RNA NORAD protects against cerebral ischemia/reperfusion injury induced brain damage, cell apoptosis, oxidative stress and inflammation by regulating miR-30a-5p/YWHAG. Bioengineered 2021; 12: 9174-88.
7. Wu MY, Yiang GT, Liao WT, et al. Current mechanistic concepts in ischemia and reperfusion injury. Cell Physiol Biochem 2018; 46: 1650-67.
8. Herpich F, Rincon F. Management of acute ischemic stroke. Crit Care Med 2020; 48: 1654-63.

9. Amani H, Mostafavi E, Alebouyeh MR, et al. Would colloidal gold nanocarriers present an effective diagnosis or treatment for ischemic stroke? Int J Nanomed 2019; 14: 8013-31.
10. Zhu XN, Li J, Qiu GL, et al. Propofol exerts anti-anhedonia effects via inhibiting the dopamine transporter. Neuron 2023; 111: 1626-36 e6.
11. Guo XN, Ma X. The effects of propofol on autophagy. DNA Cell Biol 2020; 39: 197-209.
12. Fan W, Zhu X, Wu L, et al. Propofol: an anesthetic possessing neuroprotective effects. Eur Rev Med Pharmacol Sci 2015; 19: 1520-9.
13. Tao W, Zhang X, Ding J, et al. The effect of propofol on hypoxia- and TNF-α-mediated BDNF/TrkB pathway dysregulation in primary rat hippocampal neurons. CNS Neurosci Ther 2022; 28: 761-74.
14. Engelhard K, Werner C, Eberspächer E, et al. Influence of propofol on neuronal damage and apoptotic factors after incomplete cerebral ischemia and reperfusion in rats: a long-term observation. Anesthesiology 2004; 101: 912-7.
15. Huang L, Ding L, Yu S, Huang X, Ren Q. Propofol postconditioning alleviates diabetic myocardial ischemia-reperfusion injury via the miR-200c-3p/AdipoR2/STAT3 signaling pathway. Mol Med Rep 2022; 25: 137.
16. Zhou R, Yang Z, Tang X, Tan Y, Wu X, Liu F. Propofol protects against focal cerebral ischemia via inhibition of microglia-mediated proinflammatory cytokines in a rat model of experimental stroke. PLoS One 2013; 8: e82729.
17. Gao X, Mi Y, Guo N, et al. The mechanism of propofol in cancer development: an updated review. Asia Pac J Clin Oncol 2020; 16: e3-11.
18. Feng L, Sun ZG, Liu QW, et al. Propofol inhibits the expression of Abelson nonreceptor tyrosine kinase without affecting learning or memory function in neonatal rats. Brain Behav 2020; 10: e01810.
19. Romuk EB, Szczurek W, Nowak PG, Hudziec E, Chwalińska E, Birkner E. Effects of propofol on the liver oxidative-antioxidant balance in a rat model of Parkinson's disease. Adv Clin Exp Med 2016; 25: 815-20.
20. Yu W, Gao D, Jin W, Liu S, Qi S. Propofol prevents oxidative stress by decreasing the ischemic accumulation of succinate in focal cerebral ischemia-reperfusion injury. Neurochem Res 2018; 43: 420-9.
21. Jia L, Wang F, Gu X, et al. Propofol postconditioning attenuates hippocampus ischemia-reperfusion injury via modulating JAK2/STAT3 pathway in rats after autogenous orthotropic liver transplantation. Brain Res 2017; 1657: 202-7.
22. Chen Y, Li Z. Protective effects of propofol on rats with cerebral ischemia-reperfusion injury via the PI3K/Akt pathway. J Mol Neurosci 2021; 71: 810-20.
23. Hausburg MA, Banton KL, Roman PE, et al. Effects of propofol on ischemia-reperfusion and traumatic brain injury. J Crit Care 2020; 56: 281-7.
24. Zhang Y, Yuan X, Xu J, Gu H. CircRBM33 induces endothelial dysfunction by targeting the miR-6838-5p/PDCD4 axis affecting blood-brain barrier in mice with cerebral ischemia-reperfusion injury. Clin Hemorheol Microcirc 2023; 85: 355-70.
25. Morishita Y, Matsuzaki T, Hara-chikuma M, et al. Disruption of aquaporin-11 produces polycystic kidneys following vacuolization of the proximal tubule. Mol Cell Biol 2005; 25: 7770-9.
26. Gorelick DA, Praetorius J, Tsunenari T, et al. Aquaporin-11: a channel protein lacking apparent transport function expressed in brain. BMC Biochem 2006; 7: 14.
27. Zuo ML, Wang AP, Song GL, Yang ZB. miR-652 protects rats from cerebral ischemia/reperfusion oxidative stress injury by directly targeting NOX2. Biomed Pharmacother 2020; 124: 109860.
28. Sun B, Ou H, Ren F, Guan Y, Huan Y, Cai H. Propofol protects against cerebral ischemia/reperfusion injury by down-regulating long noncoding RNA SNHG14. ACS Chem Neurosci 2021; 12: 3002-14.
29. Liang C, Cang J, Wang H, Xue Z. Propofol attenuates cerebral ischemia/reperfusion injury partially using heme oxygenase-1. J Neurosurg Anesthesiol 2013; 25: 311-6.
30. Sun B, Ou H, Ren F, et al. Propofol protects against cerebral ischemia/reperfusion injury by down-regulating long noncoding RNA SNHG14. ACS Chem Neurosci 2021; 12: 3002-14.
31. Lu Y, Han Y, He J, Zhou B, Fang P, Li X. LncRNA FOXD3-AS1 knockdown protects against cerebral ischemia/reperfusion injury via miR-765/BCL2L13 axis. Biomed Pharmacother 2020; 132: 110778.
32. Wang C, Hu F. Long noncoding RNA SOX2OT silencing alleviates cerebral ischemia-reperfusion injury via miR-135a-5p-mediated NR3C2 inhibition. Brain Res Bull 2021; 173: 193-202.
33. Yang B, Zang LE, Cui JW, Zhang MY, Ma X, Wei LL. Melatonin plays a protective role by regulating miR-26a-5p-NRSF and JAK2-STAT3 pathway to improve autophagy, inflammation and oxidative stress of cerebral ischemia-reperfusion injury. Drug Des Devel Ther 2020; 14: 3177-88.
34. Hu Y, Ye C, Cheng S, Chen J. Propofol downregulates lncRNA MALAT1 to alleviate cerebral ischemia-reperfusion injury. Inflammation 2021; 44: 2580-91.
35. Chen C, Chang X, Zhang S, Zhao Q, Lei C. CircRNA CTNNB1 (circCTNNB1) ameliorates cerebral ischemia/reperfusion injury by sponging miR-96-5p to up-regulate scavenger receptor class B type 1 (SRB1) expression. Bioengineered 2022; 13: 10258-73.
36. Li J, He W, Wang Y, Zhao J, Zhao X. miR-103a-3p alleviates oxidative stress, apoptosis, and immune disorder in oxygen-glucose deprivation-treated BV2 microglial cells and rats with cerebral ischemia-reperfusion injury by targeting high mobility group box 1. Ann Transl Med 2020; 8: 1296.
37. Kuai F, Zhou L, Zhou J, Sun X, Dong W. Long non-coding RNA THRIL inhibits miRNA-24-3p to upregulate neuropilin-1 to aggravate cerebral ischemia-reperfusion injury through regulating the nuclear factor κB p65 signaling. Aging 2021; 13: 9071-84.
38. Wang B, Chen S, Yang J, Yang L, Liu J, Zhang W. ET-26 hydrochloride (ET-26 HCl) has similar hemodynamic stability to that of etomidate in normal and uncontrolled hemorrhagic shock (UHS) rats. PLoS One 2017; 12: e0183439.
39. Liu H, Wu X, Luo J, et al. Adiponectin peptide alleviates oxidative stress and NLRP3 inflammasome activation after cerebral ischemia-reperfusion injury by regulating AMPK/GSK-3β. Exp Neurol 2020; 329: 113302.
40. Liang Q, Yang J, He J, et al. Stigmasterol alleviates cerebral ischemia/reperfusion injury by attenuating inflammation and improving antioxidant defenses in rats. Biosci Rep 2020; 40: BSR20192133.
41. Leech T, Chattipakorn N, Chattipakorn SC. The beneficial roles of metformin on the brain with cerebral ischaemia/reperfusion injury. Pharmacol Res 2019; 146: 104261.
42. Lu TX, Rothenberg ME. MicroRNA. J Allergy Clin Immunol 2018; 141: 1202-7.

43. Xing F, Liu Y, Dong R, Cheng Y. miR-374 improves cerebral ischemia reperfusion injury by targeting Wnt5a. Exp Anim 2021; 70: 126-36.
44. Lu MY, Wu JR, Liang RB, et al. Upregulation of miR-219a-5p decreases cerebral ischemia/reperfusion injury in vitro by targeting Pde4d. J Stroke Cerebrovasc Dis 2020; 29: 104801.
45. Jiang F, Liu X, Wang X, Hu J, Chang S, Cui X. LncRNA FGD5-AS1 accelerates intracerebral hemorrhage injury in mice by adsorbing miR-6838-5p to target VEGFA. Brain Res 2022; 1776: 147751.
46. Zhang G, Ding L, Sun G, et al. LncRNA AZIN1-AS1 ameliorates myocardial ischemia-reperfusion injury by targeting miR-6838-5p/WNT3A axis to activate Wnt-β/catenin signaling pathway. In Vitro Cell Dev Biol Anim 2022; 58: 54-68.
47. Bartel DP. MicroRNAs: genomics, biogenesis, mechanism, and function. Cell 2004; 116: 281-97.
48. Koike S, Tanaka Y, Matsuzaki T, Morishita Y, Ishibashi K. Aquaporin-11 (AQP11) expression in the mouse brain. Int J Mol Sci 2016; 17: 861.
49. Xi T, Jin F, Zhu Y, et al. miR-27a-3p protects against blood-brain barrier disruption and brain injury after intracerebral hemorrhage by targeting endothelial aquaporin-11. J Biol Chem 2018; 293: 20041-50.
50. Su G, Qu Y, Li G, Deng M. Sevoflurane protects against cerebral ischemia/reperfusion injury via microrna-30c-5p modulating homeodomain-interacting protein kinase 1. Bioengineered 2021; 12: 11858-71.
51. Yan K, Hu C, Liu C, et al. LncRNA CERS6-AS1, sponging miR-6838-5p, promotes proliferation and invasion in cervical carcinoma cells by upregulating FOXP2. Histol Histopathol 2023; 38: 823-35.
52. Zhao X, Zhu X, Xiao C, Hu Z. LncRNA SH3BP5-AS1 promotes hepatocellular carcinoma progression by sponging miR-6838-5p and activation of PTPN4. Aging 2024; 16: 8511-23.
53. Krajčová A, Waldauf P, Anděl M, Duška F. Propofol infusion syndrome: a structured review of experimental studies and 153 published case reports. Crit Care 2015; 19: 398.